



ENG470 Engineering Honours Thesis

Model and Simulation Development for the Convective, Hot-Air Drying of In-Shell Macadamia Nuts

Author:
Mr. Mitchell Barbara

Supervisors:
Prof. Parisa A. Bahri
Dr. Karne De Boer

Bachelor of Engineering Honours [BEng(Hons)]
“Instrumentation and Control”, “Industrial Computer Systems”

December 3rd, 2018

This page has been left blank intentionally

AUTHOR'S DECLARATION

I Mitchell Barbara confirm that the writing and research herein has been conducted entirely by myself. This thesis has not been submitted as part of any other degree or course of study at another institution. All phrasing is to the best of my knowledge entirely original, and all information is my own unless explicitly cited in text and referenced appropriately. Any figures, tables or illustrations are either reconstructed adaptations from those found in literature or entirely original. Any such reconstruction has been duly cited in text and referenced appropriately.

Word count: 15,114 words

Signed,

Date: ____/____/_____

Mr. Mitchell Barbara

ABSTRACT

The drying of agricultural food crops is an essential process in ensuring the safe and reliable delivery of produce to consumers. This is no less true for cultivated nuts, grains and seeds, which have a certain vulnerability to degradation under moist conditions. The macadamia nut is particularly susceptible to this issue, due to its high oil content and markedly slow drying characteristics, providing rancidity and disease with an opportunity to spoil the produce. In recent decades, the design of efficient industrial drying schemes has become a large focus for researchers, with many studies aiming to better describe the underlying physical processes in food drying. This dissertation details the design and implementation of a fundamental model and accompanying simulation for the drying of nut-in-shell macadamias, intended to aid a future control system design study.

Research is given toward the macadamia industry, as well as some of the relevant physical properties of the nut. An extensive review is given on modelling, with particular importance placed on techniques used for the deep-bed drying of nuts, grains and seeds. Control system architecture is briefly discussed, but is not the primary focus of this report. Verification of work done by prior researchers is carried out, before then deriving a comprehensive deep-bed drying model for macadamias. Crucial aspects toward how such a model is adapted into a MATLAB simulation is given, without intending to become an extensive review on software design. A robust and thorough model verification procedure is conducted, to prove that the final simulation does indeed successfully suit the purposes of control system design.

ACKNOWLEDGEMENTS

Firstly, I would like to thank my two project supervisors Prof. Parisa A. Bahri and Dr. Karne De Boer for their guidance, support and stewardship throughout the duration of this project. It has been a long and difficult journey, but their help has been instrumental to its success. I would also like to thank Andras Nagy for his help with acquiring plant data and process information, and simply shooting the breeze about the particulars of macadamia nut drying. I have to thank my family and friends for supporting me throughout all of my studies; for celebrating my victories and pushing me to work hard and challenge myself. A special mention should go to Joseph Allsop for his advice on discretisation methods when MATLAB chose to be deceitful. Perhaps most importantly, I wish to thank the entire engineering staff at Murdoch University. Your gifts of knowledge and support over the last 4 years is something I cherish; thank you for helping me become a better student and engineer.

- Mitch

TABLE OF CONTENTS

Author’s Declaration	i
Abstract.....	ii
Acknowledgements.....	iii
List of Figures	vii
List of Tables	viii
List of Equations.....	viii
Nomenclature	xi
Chapter 1: Introduction	1
Chapter 2: Macadamia Nuts and Agriculture	4
2.1 Physical Properties of Macadamia Nuts	4
2.1.1 Moisture Sorption Characteristics	4
2.2 Post-Harvest Processes	7
2.2.1 The Drying Process.....	7
2.3 Ensuring Product Quality	9
Chapter 3: Modelling Food Drying Processes	11
3.1 Fundamental Mechanisms to Drying.....	11
3.2 Thin-Layer Modelling	12
3.3 Deep-Bed Modelling	14
3.3.1 Sample Modelling Procedure.....	15
3.4 Simulation	18
Chapter 4: Control System Architecture.....	21

4.1	Process Control for Food Drying	21
4.2	Control Strategies for Macadamia Drying.....	22
Chapter 5:	Verifying the Literature	24
5.1	NIS Macadamia Thin-Layer Drying Characteristics	24
5.2	Hazelnut Deep-Bed Drying Simulation.....	26
Chapter 6:	Model Construction	31
6.1	Design, Layout and structure	31
6.2	Subsidiary Process Models.....	33
6.2.1	Inlet Air Mixing Process.....	33
6.2.2	Inlet Air Heat Exchanger Process	36
6.3	Simulation Development	39
6.3.1	Constructing the Deep-Bed Simulation.....	39
6.3.2	Implementing Subsidiary Processes.....	41
6.3.3	Finalised Open-Loop Simulation	45
Chapter 7:	Model Verification	51
7.1	Data Cleansing.....	51
7.2	Validation of Model Outputs	55
7.2.1	NIS Macadamia Drying Process.....	55
7.2.2	Inlet Air Conditions	60
Chapter 8:	Conclusion.....	63
8.1	Issues, Challenges and Barriers.....	63
8.2	Future Works	64

8.2.1	Improving the Model and Simulation	64
8.2.2	Control System Design	65
8.3	Concluding Remarks.....	68
	Bibliography	71
	Appendix	76
A.	Novel Drying Technologies.....	76
B.	Using the System Identification Toolbox	77
C.	Approximating the Equivalent Drying Time	83

LIST OF FIGURES

FIGURE 1: MACADAMIA SUPPLY CHAIN - YEAR ENDING JUNE 2016 [2]	1
FIGURE 2: MACADAMIA NUT DESORPTION ISOTHERM [11]	5
FIGURE 3: VARIATION IN LATENT HEAT OF WATER IN MACADAMIA NUTS AGAINST THE LATENT HEAT OF WATER IN AIR AS A FUNCTION OF NUT MOISTURE CONTENT (%W.B.) [11].....	6
FIGURE 4: SAMPLE DEEP-BED DRYING SYSTEM P&ID	8
FIGURE 5: ELEMENTAL THIN-LAYER BREAKDOWN [22]	14
FIGURE 6: MOISTURE BALANCE GUIDING PRINCIPLE [23].....	15
FIGURE 7: HEAT BALANCE GUIDING PRINCIPLE [23].....	15
FIGURE 8: HEAT TRANSFER GUIDING PRINCIPLE [23].....	16
FIGURE 9: LOGIC FLOW CHART FOR A DISCRETE DEEP-BED HAZELNUT SIMULATION [21].....	19
FIGURE 10: LOGIC FLOW DIAGRAM FOR THIN-LAYER MODEL VERIFICATION	25
FIGURE 11: VERIFICATION OF OPEN LOOP RESPONSE FOR THIN-LAYER MODEL.....	26
FIGURE 12: VERIFICATION OF CHANGES IN PRODUCT MOISTURE CONTENT FOR DEEP-BED SIMULATIONS.....	30
FIGURE 13: OVERALL OPEN-LOOP PROCESS BLOCK DIAGRAM.....	32
FIGURE 14: DIAGRAM OF THE INLET AIR MIXING POINT	34
FIGURE 15: COMPARISON OF AIRFLOW FOR FULLY OPEN AND FULLY CLOSED INLET DAMPER POSITIONS.....	34
FIGURE 16: HEAT EXCHANGER APPROXIMATED MODEL STRUCTURE	37
FIGURE 17: STEP RESPONSE OF CONTINUOUS, DISCRETE AND DIFFERENCE MODEL VARIANTS.....	43
FIGURE 18: COMPARISON OF AN ANALYTICALLY DERIVED DIFFERENCE EQUATION TO ITS CONTINUOUS TIME TRANSFER FUNCTION FOR THE HEAT EXCHANGER APPROXIMATE MODEL.....	45
FIGURE 19: LOGIC FLOW DIAGRAM FOR OPEN-LOOP SIMULATION	46
FIGURE 20: OPEN-LOOP SIMULATION #1 - PROCESS REACTIONS	48
FIGURE 21: OPEN-LOOP SIMULATION #2 - PROCESS REACTIONS	49
FIGURE 22: OPEN-LOOP SIMULATION #3 - PROCESS REACTIONS	50
FIGURE 23: SNAPSHOT OF RAW PLANT DATA FORMATTING	52
FIGURE 24: FILTERING OF NOISY DATA FOR THE USE IN MATLAB'S SYSTEM IDENTIFICATION TOOLBOX	54
FIGURE 25: DIFFERENCE BETWEEN INTERPOLATION AND A ZERO-ORDER-HOLD	54

FIGURE 26: RH (LEFT) AND TEMPERATURE (RIGHT) VALIDATION CURVES; SILOS 15 AND 21, BATCHES 100, 112 AND 127	56
FIGURE 27: RH (LEFT) AND TEMPERATURE (RIGHT) VALIDATION CURVES; SILOS 22, 23 AND 24, BATCHES 097, 109 AND 128	57
FIGURE 28: COMPARISON OF THE TEMPERATURE GRADIENT EXHIBITED BY PLANT DATA VS MODEL DATA	59
FIGURE 29: INLET AIR MODEL VALIDATION DATA COMPARISON	61
FIGURE 30: EXAMPLE RESPONSE FOR A CLOSED-LOOP CONVENTIONAL FEEDBACK CONTROL SCENARIO ($K_C = 0.10521$, $\tau_{U_i} = 267.5056$, $\tau_{U_D} = 0$)	67
FIGURE 31: MATLAB SYSTEM IDENTIFICATION TOOLBOX GUI	79
FIGURE 32: IDENT IMPORT DATA GUI	80
FIGURE 33: IDENT SELECT RANGE GUI	81
FIGURE 34: IDENT MODEL OUTPUT GUI	82
FIGURE 35: IDENT PROCESS MODELS GUI	82
FIGURE 36: CHANGES IN EQUIVALENT DRYING TIME OVER ACTUAL DRYING TIME	83
FIGURE 37: PIECEWISE LINEAR APPROXIMATION OF CHANGES IN EQUIVALENT DRYING TIME	84

LIST OF TABLES

TABLE 1: DATA USED FOR VERIFICATION OF THE DEEP-BED ALGORITHM [21]	27
TABLE 2: FAILED HEAT EXCHANGER EMPIRICAL MODEL STRUCTURES	37
TABLE 3: CONSTANT SYSTEM PARAMETERS FOR SIMULATION	47
TABLE 4: OPEN-LOOP SIMULATION - PROCESS PARAMETERS	47
TABLE 5: QUANTIFIED PERFORMANCE DATA FOR RH MODEL ACCURACY	58
TABLE 6: QUANTIFIED PERFORMANCE DATA FOR TEMPERATURE MODEL ACCURACY	60

LIST OF EQUATIONS

EQUATION (2.1): EQUILLIBRIUM MOISTURE CONTENT (GAB EQUATION)	5
EQUATION (2.2): GAB COEFFICIENT Y	5
EQUATION (2.3): GAB COEFFICIENT K	5

EQUATION (2.4): GAB COEFFICIENT W_m	6
EQUATION (2.5): LATENT HEAT RATIO OF THE PRODUCT TO WATER IN AIR	6
EQUATION (3.1): TWO-TERM EXPONENTIAL THIN-LAYER DRYING MODEL	13
EQUATION (3.2): THIN-LAYER DRYING MODEL COEFFICIENT K_1	13
EQUATION (3.3): MOISTURE BALANCE PDE	15
EQUATION (3.4): HEAT BALANCE PDE	16
EQUATION (3.5): HEAT TRANSFER PDE	16
EQUATION (3.6): VOLUMETRIC HEAT TRANSFER COEFFICIENT BY CONVECTION	16
EQUATION (3.7): MOISTURE CONTENT FINITE DIFFERENCE SOLUTION	16
EQUATION (3.8): HEAT BALANCE FINITE DIFFERENCE SOLUTION	17
EQUATION (3.9): HEAT TRANSFER FINITE DIFFERENCE SOLUTION	17
EQUATION (3.10): HEAT TRANSFER COEFFICIENT A	17
EQUATION (3.11): HEAT TRANSFER COEFFICIENT B	17
EQUATION (3.12): HEAT TRANSFER COEFFICIENT E	17
EQUATION (3.13): HEAT TRANSFER COEFFICIENT F	17
EQUATION (3.14): HEAT TRANSFER COEFFICIENT Y	17
EQUATION (5.1): PAGE'S THIN-LAYER DRYING MDOEL	27
EQUATION (5.2): PAGE MODEL COEFFICIENT k	27
EQUATION (5.3): PAGE MODEL COEFFICIENT n	27
EQUATION (5.4): DERIVATIVE OF PAGE'S THIN-LAYER MODEL	28
EQUATION (5.5): PAGE MODEL FINITE DIFFERENCE SOLUTION	28
EQUATION (5.6): PAGE MODEL EQUIVALENT DRYING TIME	28
EQUATION (5.7): PAGE MODEL FINITE DIFFERENCE SOLUTION INCORPORATING t_{eq}	28
EQUATION (5.8): LATENT HEAT OF VAPORISATION OF WATER IN A HAZELNUT	29
EQUATION (5.9): LATENT HEAT OF VAPORISATION OF WATER IN AIR	29
EQUATION (5.10): SATURATION VAPOUR PRESSURE OF AIR	29
EQUATION (5.11): APPARENT MOISTURE CONTENT OF AIR	29
EQUATION (5.12): ALTERNATIVE SOLUTION FOR THE SATURATION VAPOUR PRESSURE OF AIR	29
EQUATION (6.1): INLET MIXING POINT TEMPERATURE COMPONENT BALANCE	35

EQUATION (6.2): INLET MIXING POINT TEMPERATURE COMPONENT BALANCE (WITH DAMPER).....	35
EQUATION (6.3): MIXING POINT OUTLET TEMPERATURE.....	35
EQUATION (6.4): HUMIDITY RATIO.....	35
EQUATION (6.5): HUMIDITY RATIO VIA PARTIAL PRESSURE OF WATER VAPOUR.....	35
EQUATION (6.6): PARTIAL PRESSURE OF WATER VAPOUR.....	36
EQUATION (6.7): INLET MIXING POINT HUMIDITY RATIO COMPONENT BALANCE	36
EQUATION (6.8): INLET MIXING POINT HUMIDITY RATIO COMPONENT BALANCE (WITH DAMPER)	36
EQUATION (6.9): MIXING POINT OUTLET HUMIDITY RATIO	36
EQUATION (6.10): PARTIAL PRESSURE OF WATER VAPOUR VIA HUMIDITY RATIO	36
EQUATION (6.11): RELATIVE HUMIDITY VIA PARTIAL PRESSURE OF WATER VAPOUR.....	36
EQUATION (6.12): HEAT EXCHANGER'S EMPIRICAL APPROXIMATE MODEL.....	38
EQUATION (6.13): DERIVATIVE OF TWO-TERM EXPONENTIAL THIN-LAYER DRYING MODEL.....	40
EQUATION (6.14):TWO-TERM EXPONENTIAL DRYING MODEL FINITE DIFFERENCE SOLUTION.....	40
EQUATION (6.15): LATENT HEAT OF VAPORISATION OF WATER IN A MACADAMIA NUT.....	41
EQUATION (6.16): HEAT EXCHANGER CONTINUOUS TIME TRANSFER FUNCTION.....	41
EQUATION (6.17): HEAT EXCHANGER PULSE TRANSFER FUNCTION.....	42
EQUATION (6.18): HEAT EXCHANGER DIFFERENCE EQUATION.....	42
EQUATION (6.19): HEAT EXCHANGER CONTINUOUS TIME TRANSFER FUNCTION (GENERALISED).....	43
EQUATION (6.20): HEAT EXCHANGER CONTINUOUS TIME TRANSFER FUNCTION (WORKING 1).....	44
EQUATION (6.21): HEAT EXCHANGER CONTINUOUS TIME TRANSFER FUNCTION (WORKING 2).....	44
EQUATION (6.22): HEAT EXCHANGER DIFFERENCE EQUATION (WORKING)	44
EQUATION (6.23): HEAT EXCHANGER DIFFERENCE EQUATION.....	44
EQUATION (6.24): HEAT EXCHANGER COEFFICIENT A	44
EQUATION (6.25): HEAT EXCHANGER COEFFICIENT B	44
EQUATION (6.26): HEAT EXCHANGER COEFFICIENT C	44
EQUATION (6.27): HEAT EXCHANGER COEFFICIENT D	44
EQUATION (10.1): EQUIVALENT DRYING TIME GRADIENT PIECEWISE APPROXIMATION	84
EQUATION (10.2): EQUIVALENT DRYING TIME DIFFERENCE PIECEWISE APPROXIMATION	84

NOMENCLATURE

Abbreviations

AI	Artificial Intelligence
ANN	Artificial Neural Network
ANFIS	Adaptive Neuro-Fuzzy Inference System
APC	Advanced Process Control
ARX	Autoregressive with Exogenous Terms [Model]
.csv	Comma Separated Value
D.B.	Dry Basis
DMC	Dynamic Matrix Control
FFA	Fatty Free Acid
GAB	Guggenheim-Anderson-De Boer
GMC	Generic Model Control
GUI	Graphical User Interface
HE	Heat Exchanger
IDENT	MATLAB System Identification Toolbox
NIS	Nut-In-Shell
MATLAB	Matrix Laboratory (by MathWorks, Inc.)
MFNN	Multilayer Feedforward Neural Network
MPC	Model Predictive Control
MS	Microsoft, Inc.
MV	Manipulated Variable
PDE	Partial Differential Equation
PID	Proportional Integral Derivative
P&ID	Process and Instrument Diagram

PLC	Programmable Logic Controller
PV	Process Variable
RF	Radio Frequency
RH	Relative Humidity
SISO	Single Input, Single Output
Temp	Temperature
VPN	Virtual Private Network
VSD	Variable Speed Drive
W.B.	Wet Basis
ZOH	Zero-Order Hold

Algebraic Symbols

A_p	Heat transfer surface area of the product	(m^2)
a_w	Water activity of air	-
C_a	Specific heat capacity of air	$(KJ/Kg^{\circ}C)$
C_p	Specific heat capacity of the product	$(KJ/Kg^{\circ}C)$
C_v	Specific heat capacity of water vapour in air	$(KJ/Kg^{\circ}C)$
C_w	Specific heat capacity of water	$(KJ/Kg^{\circ}C)$
D	Damper Position	-
G	Flow rate of air	$(Kg/s.m^2)$
G_{HE}	Heat exchanger continuous transfer function	-
h_c	Heat transfer coefficient by convection	$(KW/m^2^{\circ}C)$
K_p	Heat exchanger process gain	-
L_a	Latent heat of water in air	(KJ/Kg)
L_p	Latent heat of water in the product	(KJ/Kg)

M	Moisture content of the product	$(Kg_{water}/Kg_{dry\ matter})$
$M_{\%}$	Moisture content of the product (percentage)	(%)
M_e	Equilibrium moisture content of the product	$(Kg_{water}/Kg_{dry\ matter})$
M_o	Initial moisture content of the product	$(Kg_{water}/Kg_{dry\ matter})$
M_w	Content of water vapour in air	(Kg_{water})
P	Total air pressure	(Pa)
P_s	Saturation vapour pressure	(Pa)
P_w	Partial pressure of water vapour in air	(Pa)
RH	Relative humidity of air	(%)
t	Time	(s)
t_{eq}	Equivalent drying time	(s)
T_a	Air temperature	$(^{\circ}C)$
T_A	Ambient air temperature	$(^{\circ}C)$
T_f	Temperature of mixing point outlet air	$(^{\circ}C)$
T_{out}	Outlet air temperature of the heat exchanger	$(^{\circ}C)$
T_p	Temperature of the product	$(^{\circ}C)$
T_R	Recycled air temperature	$(^{\circ}C)$
τ_{p1}	Heat exchanger process time constant 1	-
τ_{p1}	Heat exchanger process time constant 2	-
τ_z	Heat exchanger process zero	-
U_{HE}	Heat exchanger control valve position	-
\dot{V}_A	Volumetric flowrate of ambient air	(m^3/s)
\dot{V}_R	Volumetric flowrate of recycled air	(m^3/s)
w_a	Moisture content of the air	$(Kg_{water}/Kg_{dry\ air})$
W	Humidity Ratio	$(Kg_{water}/Kg_{dry\ matter})$

W_A	Ambient air humidity ratio	$(Kg_{water}/Kg_{dry\ air})$
W_f	Humidity ratio of mixing point outlet air	$(Kg_{water}/Kg_{dry\ air})$
W_m	Mono-layer moisture content	$(Kg_{water}/Kg_{dry\ matter})$
W_R	Recycled air humidity ratio	$(Kg_{water}/Kg_{dry\ air})$
Y_{HE}	Heat exchanger temperature addition via valve	$(^{\circ}C)$
z	Position of an elementary layer within the bed of product	(m)
ρ_a	Density of air	$(Kg_{dry\ air}/m^3)$
ρ_p	Density of the product	$(Kg_{dry\ matter}/m^3)$
ε	Porosity	-

Chapter 1: INTRODUCTION

For many years the Australian economy has benefited from strength in the export of resources, livestock and agricultural produce. It is interesting to note however, that there has only ever been one natively Australian food crop to be commercially exported overseas, namely the macadamia nut [1]. With over 700 growers servicing 40 countries, the Australian macadamia industry is recognised as a global market leader [1], exporting over 70% of its total yield to overseas customers [2]. In 2017 the Australian macadamia industry reportedly produced 46,000 metric tonnes of in-shell macadamia nuts at a farm-gate average value of \$5.62 per Kg – equating to over \$252M in gross revenue [3]. Although, the wholesale value of nuts remains at a lesser \$89M [2], highlighting the large capital overhead in production and processing. This overhead has provided pressure on the industry to continually innovate and refine the harvest and production process, with Australian growers investing approximately \$2M each year on research [1]. Horticulture Innovation Australia [2] provided information showing the macadamia supply chain for the 2015/16 financial year (Figure 1), showing the flow of production to consumers.

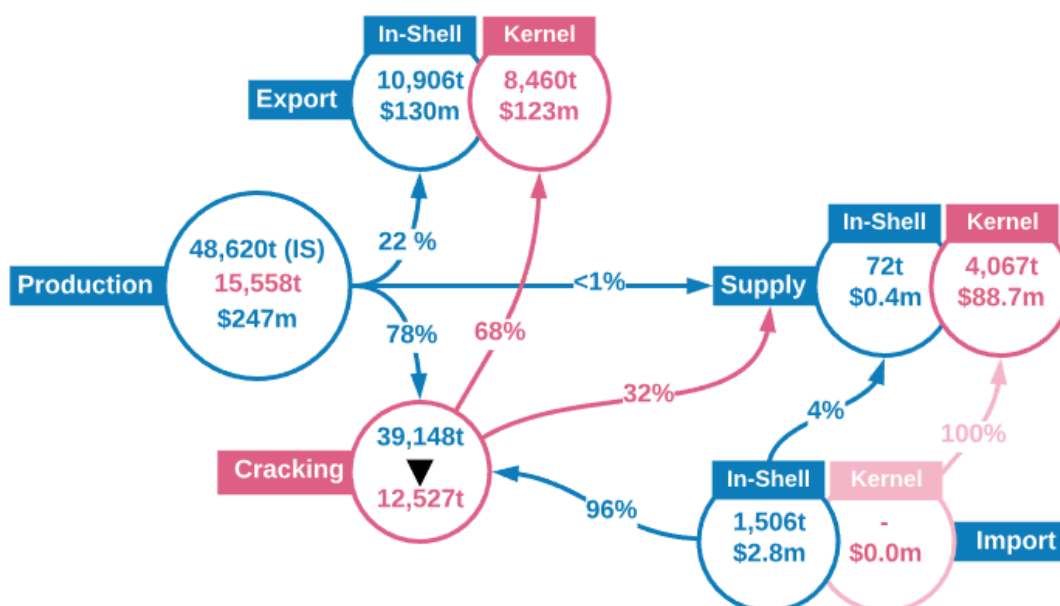


Figure 1: Macadamia supply chain - year ending June 2016 [2]

Macadamias are a highly perishable food [4], with stringent storage requirements to ensure the product remains safe to eat well after delivery to consumers [5]. Perhaps the most crucial aspect in guaranteeing a high-quality yield is to lower the product's moisture content, preventing disease and rancidity. Various drying techniques have been employed and tested over recent decades, with the industry converging towards convective, hot-air drying as the most suitable for the application [6]. This process can be expensive, lengthy and fastidious, attributable to approximately 12-20% of the manufacturing industry's energy consumption [4]. From a process control perspective, these systems are not overly complicated. Yet defining the underlying physical process which occurs during drying has been a hot topic for many researchers, in an effort to derive an accurate process model. These models can facilitate the development of simulations which assist in the design of optimal drying regimes. Any successful regime is often subject to well-known heuristics which aim to ensure the product remains at a certain quality whilst drying.

Throughout this report, the various aspects toward modelling a macadamia nut drying process will be presented. There are some unique techniques used for the drying of nuts, grains and seeds which will be reviewed. Just as significant will be discussions given toward how such a model may be implemented into a simulated programming environment. Thus the aims of this study are stated to be:

- To develop a suitable process model which – wherever possible – uses fundamental physical phenomena to adequately describe the dynamics of a macadamia drying system;
- To adapt this model into a discrete MATLAB simulation, intended for use in a future control system design study.

It is not the intention of this report to provide a detailed coding tutorial, so a focus will be given toward the concepts “under the hood”, and not the specific lines of code which make up a simulation. Nevertheless, all program code will be supplied and submitted electronically.

The report opens with a background discussion arising from research and literature, laying a foundation for later chapters to build upon the work of others. Modelling will be an extensively reviewed topic, with an importance placed on drying mechanisms and theory. The model components found within literature have been reconstructed and verified before adaptation into the work of this project. The modelling and development of this simulation has been discussed at length, with any assumptions and approximations being duly noted. A rigorous validation procedure has been conducted on the model, to ensure its operation is suitable for control system design. Finally, the summary provides a comprehensive discussion toward some of the issues faced, and areas for improvement by future collaborators.

Chapter 2: MACADAMIA NUTS AND AGRICULTURE

In order to conduct the intended engineering design tasks for this project, several fundamental topics must be reviewed. Some topics may seem trivial in isolation but are indeed essential to discussions within the forthcoming chapters. In this chapter, the relevant properties of macadamia nuts are presented, post-harvest processing is reviewed, and considerations toward product quality are given. Each section aims to communicate a relevance toward specifically *drying* the produce.

2.1 PHYSICAL PROPERTIES OF MACADAMIA NUTS

Mature in-shell macadamia nuts have a consistent spherical geometry, reaching nut-in-shell (NIS) diameters of around 18-21mm [6]. They consist of a nut kernel, shell and husk, growing from evergreen trees that are typically no more than 10m tall in a commercial orchard [6]. The kernel itself is rich in oils, with the *Macadamia Integrifolia* variant being 75-80% oil by weight [5]. This high oil content has proven to be of significance throughout commercial processing, being one of the key indicators toward nut maturity and quality. In-shell macadamia nuts retain a relatively high level of moisture (25% W.B.) after dropping to the orchard floor [7]. Free water exists in the nut as a body of moisture which may be readily removed by drying, including both absorbed and adsorbed water. Bound water however, is held in place by strong chemical forces and can only be removed with high temperatures, which would in turn diminish nut quality [5]. Macadamias have a NIS bulk density of 561 Kg/m³, and specific heat capacity of approximately 2.4 KJ/Kg°C [8].

2.1.1 Moisture Sorption Characteristics

An important concept which will be revisited in following chapters is that of an equilibrium moisture content (M_e). This quantity describes how the steady state moisture content of the nut changes with its ambient surroundings. In practice, the moisture content of both the kernel and its shell are not directly measurable. Engineers instead rely on sorption isotherms, which provide a means to infer the

nut's moisture content based on the surrounding air's relative humidity for a given temperature. It should be noted however that the term "water activity" (a_w) is used in place of relative humidity, with water activity simply being the decimal form of the latter [9, 10]. Palipane and Driscoll [11] experimentally determined the moisture adsorption and desorption isotherms for macadamia nuts using the Guggenheim-Anderson-De Boer (GAB) equation. The desorption isotherm in Figure 2 illustrates (in part) the result of this study and is essential to the discussion toward modelling soon to follow.

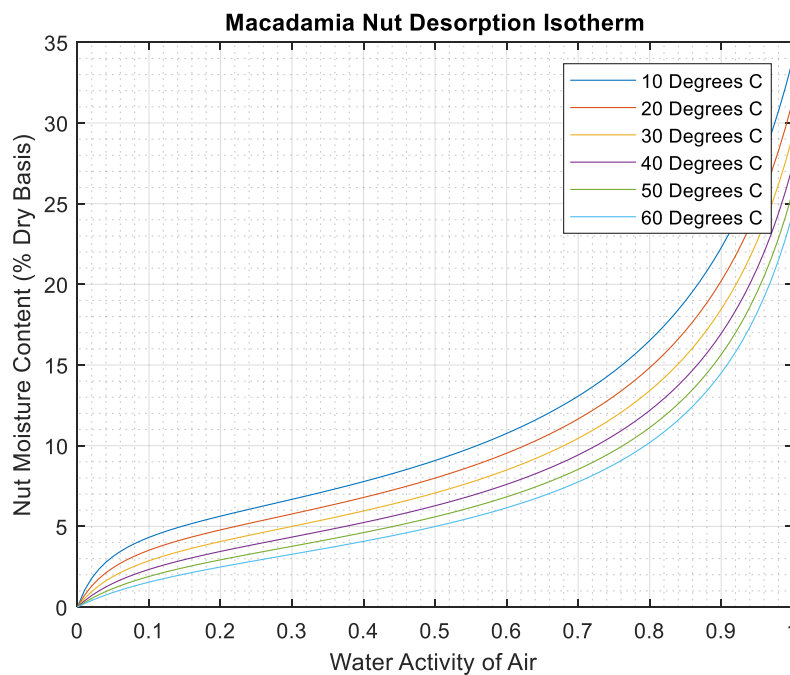


Figure 2: Macadamia nut desorption isotherm [11]

The specific equation which results in this isotherm is defined as [11]:

$$M_e = \frac{W_m Y K a_w}{[(1 - K a_w)(1 - K a_w + Y K a_w)]} \quad (2.1)$$

Where T_a is the drying air's temperature in °C and:

$$Y = 0.0069 \exp\left(\frac{2344.0}{T_a}\right) \quad (2.2)$$

$$K = 1.056 \exp\left(\frac{-65.59}{T_a}\right) \quad (2.3)$$

$$W_m = 0.1732 \exp\left(\frac{981.51}{T_a}\right) \quad (2.4)$$

Equally useful to this project is Palipane and Driscoll's derivation of the latent heat of desorption for macadamia nuts as a function of moisture content [11]. The results showed that the latent heat of the water within the nut (L_p) deviates from that of free water in air (L_a) at lower moisture contents. Figure 3 illustrates this deviation. For a nut moisture content below 20% (W.B.) the heat of desorption becomes greater than that of water alone.

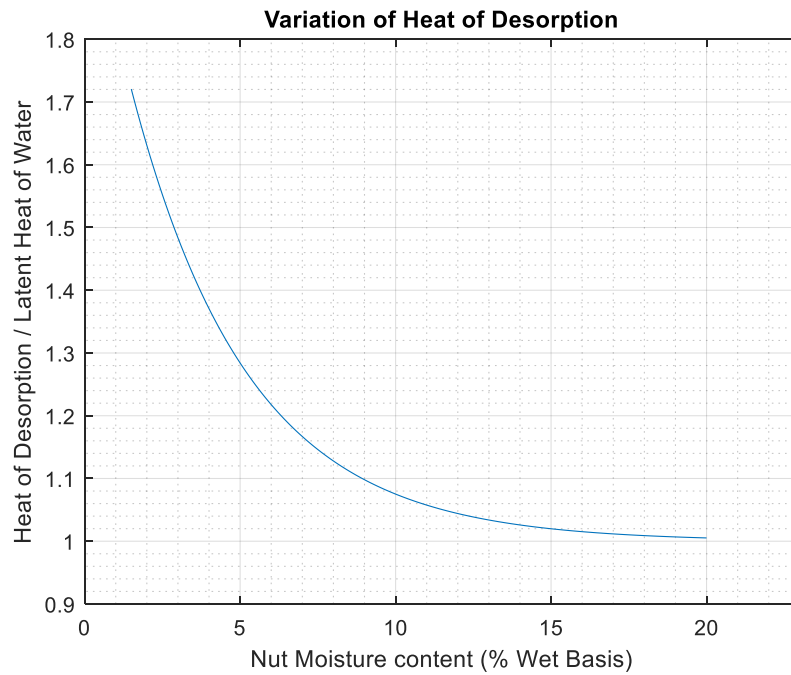


Figure 3: Variation in latent heat of water in macadamia nuts against the latent heat of water in air as a function of nut moisture content (%W.B.) [11]

The equation that provides this relationship is given by Palipane and Driscoll as [11]:

$$\frac{L_p}{L_a} = 1 + 1.074 \exp(-0.266 M_{\%}) \quad (2.5)$$

Where $M_{\%}$ is the nut moisture content as a percentage. Solving for L_p alone will give the nut's latent heat, which will be integral in modelling temperature changes in the product and required in solving the condition of the outgoing wetted air.

2.2 POST-HARVEST PROCESSES

Post-harvest processing is one of the most significant aspects to any agricultural endeavour. This is especially true for macadamia nuts, as without additional processing it would not be possible to safely deliver the product to market. Post-harvest exercises begin immediately after harvest, with dehusking occurring straight after pick-up to avoid overheating of the kernel [6]. Any twigs and stones that have made it through the cultivator should be removed before dehusking, after which any discoloured, sprouting or immature nuts should be sorted and removed [6]. Testing for maturity is particularly important, with some processors paying a premium for crops with a higher yield of mature kernels [5]. NIS testing may be done with a float test; immature, insect damaged, shrunken or degraded kernels will generally have more air in the shell and float in water [12]. However, this method does have the chance to incorrectly identify healthy nuts as defects, so a more accurate method can be performed after drying and cracking. This relies on the principle that mature kernels will have an oil content greater than 72%, implying a specific gravity less than water – causing them to float [12].

2.2.1 The Drying Process

Drying plays a critical role in the post-harvest chain of operations. It is a long and costly exercise, with the ability to foul the produce when conducted incorrectly [5]. For larger orchards, this is typically done with the use of large on-farm drying silos [12] – referred to as “Deep-Bed” drying by the scientific community. The crop’s quality will quickly deteriorate if it is not dried soon after nut-fall, so it is imperative that this be done promptly and to the right standard [7]. Figure 4 is an example Piping and Instrument Diagram (P&ID), illustrating how the on-farm drying system is typically arranged.

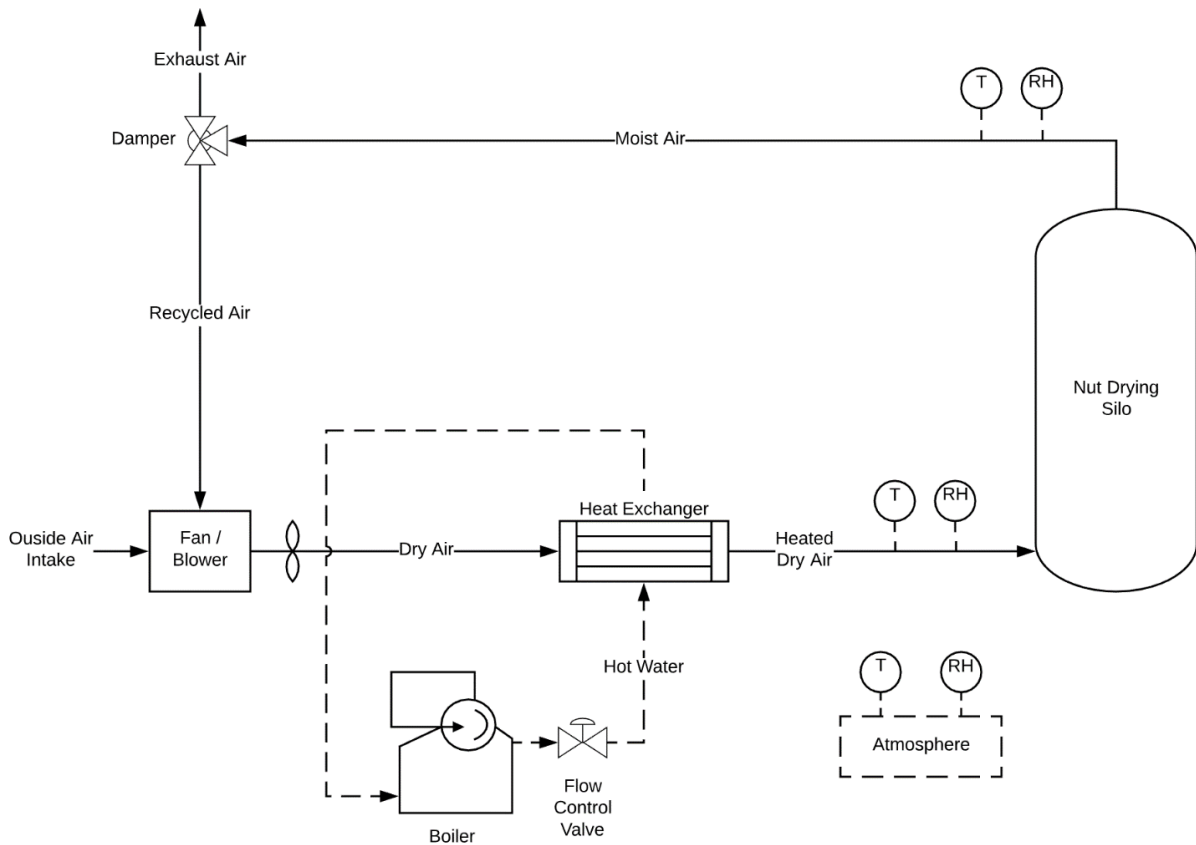


Figure 4: Sample deep-bed drying system P&ID

In the conventional example given in Figure 4, air is heated and blown through the produce to extract moisture for periods of up to 7-10 days per batch [7]. A damper can be used to recycle the wetted air for periods of high ambient relative humidity, and a flow control valve adjusts the rate of hot water being used to heat the drying air. Process feedback is provided via various sensors throughout the system, typically reading temperature and relative humidity levels at different locations. The system itself is quite simple; the real challenge however, arises in leveraging the available instrumentation to ensure efficient drying of the produce – without causing deterioration to the kernel quality [13]. A brief discussion has also been given in Appendix A which refers to some other food drying technologies, aside from the orthodox example given in Figure 4.

2.3 ENSURING PRODUCT QUALITY

Due to their high oil content and affinity for retaining moisture, product quality has become one of the most elusive aspects to macadamia production. “Unsound kernel” is a term given to the nuts which do not meet quality standards, of which there are many to consider. As discussed earlier, any cracked, germinating, sprouting or immature nuts should ideally be sorted out of the consignment early – but this alone does not guarantee a high-quality yield. The browning of kernel centres, rancidity and onset of disease all pose a threat to the produce throughout the process [6]. These defects can be much harder to diagnose and the fundamental root causes of each are still to this day debateable. What is however evident, is that drying plays a key role in reducing the occurrence of such defects [5]. More importantly, *how* drying is executed remains one of the most important considerations toward ensuring sound kernel recovery.

Conservative heating regimes should be used for initial drying periods, but the industry has yet to come to a consensus on which drying regime is ideal. Several heuristics have been suggested by different sources to ensure the produce is not overheated, but conflicting information only highlights the lack of knowledge on the issue. For example, different sources state that:

- The drying air should remain at no more than 3-4 °C [14] or 5 °C [7] above ambient temperatures.
- The drying air should not exceed 25°C [7], 30°C [15], or 38°C [14] at any time.
- The drying rate should not exceed 2% nut-in-shell moisture loss per day [15].

Other suggestions include using an incremental drying regime where the temperature is increased in stages, but this too yet remains a matter of opinion [5, 14]. High drying temperatures accompanied by high humidity is the catalyst for deterioration [7]. More aggressive heating processes like roasting should only be conducted after the product has been dried to a moisture content of about 1.5% (W.B.), as this is the point at which all free water has been removed and only bound water remains [5]. The nuts will rewet if the relative humidity of the drying air is greater than that of the nut bed, so aeration

controllers should be set up to lower the relative humidity wherever possible. The depth of the nut bed should be even across its area and not exceed 2.5m in height [7], ensuring airflow is both uniform and sufficient for all produce.

Chapter 3: MODELLING FOOD DRYING PROCESSES

The modelling of food drying processes is a well-reviewed subject, with a wide array of publications being issued for many different crops. Deriving accurate models for different processes has many benefits regarding optimisation and prediction, as well as aiding in control system design. The drying process has benefited from plentiful research, with a constant pressure for more efficient ways to dehydrate produce. This chapter aims to outline the essential prior studies relevant for the modelling and simulation of NIS macadamia drying, without becoming an exhaustive resource on the topic.

3.1 FUNDAMENTAL MECHANISMS TO DRYING

To correctly derive a dynamic model of the macadamia drying system, an understanding of the underlying transport process is required. For moist, porous produce there exist three fundamental mass transfer mechanisms: capillary flow, vapour diffusion and evaporation/condensation [16, 17]. Heat transfer is governed by the features of mass transfer, with different heat and mass transfer mechanisms being dominant at different stages in drying [16]. The heat and moisture transferred between two neighbouring particles is of a much smaller magnitude than that conducted by the drying air, so this is typically omitted from drying models [16]. Macadamia nuts are hygroscopic [11], and it has been shown that for such products, there will exist an initial constant-rate drying period, followed by subsequent falling-rate drying periods [17]. Although in practice, the nuts do not have a high enough moisture content at harvest to exhibit the constant-rate drying period.

Interestingly, it has been observed that the drying of macadamia kernels is slower than that of the in-shell counterpart [18]. This is counterintuitive, since one would assume that the shell adds an additional barrier to drying than the kernel alone. Palipane and Driscoll [18] have suggested that this may be caused by a higher moisture gradient existing across the kernel when dried alone, causing the

nut-oil to migrate to the outer layers of the kernel. The oil itself has a lower affinity to moisture than the kernel alone, so this may have a greater resistance to drying than the shell [18].

3.2 THIN-LAYER MODELLING

Thin-layer models are used in abundance within industries that conduct the drying of food. As the name implies, a thin-layer drying model aims to describe the drying characteristics of one sample layer of produce [19]. Commercially, it is inefficient to dry food in this way, but such a model provides a means for engineers to better understand how the moisture content of the produce changes under different ambient conditions [19]. Once an adequate thin-layer model has been derived, it may be used to create more complex, holistic models of the entire drying process.

There are different aspects to consider when formulating a thin-layer drying model. Different drying topologies will result in unique model equations; hence a cross-flow drying model shouldn't be attributed to a through-flow drying system [20]. For hot-air drying systems, experimental data is gathered under controlled conditions to determine a relationship (i.e. the isotherms given in Section 2.1.1) between the product's moisture content and the drying air's temperature and relative humidity [11]. The effect of the drying air's velocity is often omitted, as it can be shown for many crops that the drying air's velocity has a negligible effect on the drying rate after reaching a minor threshold [18]. The moisture content of the produce can be determined by periodically weighing the sample as it is dried, effectively inferring how much water has been evaporated during each interval [19].

Thin-layer models can be either empirical, semi-empirical or entirely theoretical in nature [19]. Purely empirical models tend to relate well to the system from which it was derived but do little to explain the fundamental transport phenomena that drive the process [17]. Furthermore, if the data used does not adequately cover a broad sample of operating conditions, then the model may not be well equipped to give an accurate description of the process [19]. In contrast to the empirical model, a

purely theoretical approach will leverage the fundamental, underlying physical processes to give a description of the system under all conditions. The downside to such an approach is that it requires an extensive understanding of the underlying processes, making it cumbersome and difficult to derive [17]. Moreover, if a system has additional, unknown phenomena affecting the process output (which may not have been captured in the model), then the model will begin to deviate from the actual process dynamics [19]. A common and indeed effective solution to the issues described above is to create a hybrid model, which adapts the theoretical approach to include empirical coefficients, tailored to the drying of specific produce [17, 19]. Such equations are usually derived from either Fick's second law of diffusion or Newton's law of cooling and can be relatively transferrable between separate systems drying the same produce [17].

Many researchers have attempted to formulate improved semi-empirical model equations, as these have become instrumental to finding accurate approximations of product moisture content [17, 19]. Palipane and Driscoll [18] conducted a study which aimed to derive a thin-layer model for the drying of in-shell macadamia nuts and kernels. Results indicated that the two-term exponential model gave an accurate description of the process under a wide array of drying conditions and has since been cited in the works of many later researchers.

$$\frac{M - M_e}{M_0 - M_e} = c_1 \exp(-k_1 t) + c_2 \exp(-k_2 t) \quad (3.1)$$

Where M_0 is the initial nut moisture content, t is time in seconds;

$$k_i = a_i \exp\left(\frac{-b_i}{T_a}\right) \quad (3.2)$$

And for NIS macadamias:

$c_1 = 0.4554$	$c_2 = 0.4993$
$a_1 = 53038.8$	$a_2 = 899.5$
$b_1 = 5110.4$	$b_2 = 4560.8$

This thin-layer model would be helpful in the derivation of a holistic “deep-bed” algorithm, which will aim to describe the characteristics of a commercial drying process.

3.3 DEEP-BED MODELLING

Unlike a thin-layer model, the deep-bed counterpart is concerned with the drying characteristics of an entire batch of produce. Such a model requires consideration to not only how the product dries, but how that affects the drying air as it progressively moves through the apparatus. Deep-bed models are typically constructed under the assumption that the bed itself contains a series of elementary thin-layers [21, 22], highlighting the utility of the discussion given in Section 3.2. Thus, by solving the conditions for the outgoing air of a given layer, the incoming air for the succeeding layer is inherently found. Assuming that at least initially the drying air is warmer than the product, then heat will be transferred to the latter – raising its temperature [16, 23]. Also, the mass of the product will change as its moisture content is reduced, in turn affecting the mass and moisture content of the drying air [16, 23]. An example breakdown of an elementary layer is given in Figure 5.

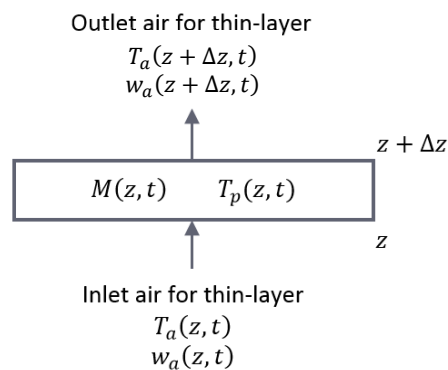


Figure 5: Elemental thin-layer breakdown [22]

3.3.1 Sample Modelling Procedure

Lopez et al. [23] published an article which walked through the steps in deriving a deep-bed drying model for malt, which then preceded a follow-up publication regarding the drying of hazelnuts [21]. The latter publication appears to be more useful in the adaptation toward a simulation for macadamias, but the former breaks down the derivations to be more easily digested. Istadi and Sitompul [22] provided a comprehensive explanation into how deep-bed models are derived, walking through the governing momentum, mass and energy conservation principles to arrive at the final balance equations. But in the interest of relevance and brevity, the following derivations are abbreviated adaptations of the prior two resources.

A balance equation for the moisture around any given elementary layer is first derived, described as:

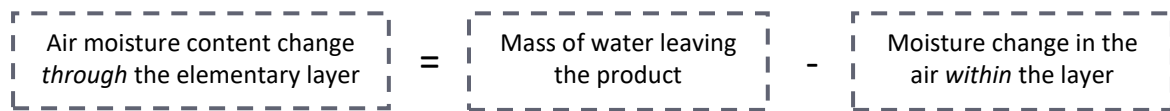


Figure 6: Moisture balance guiding principle [23]

Which is expressed as [23]:

$$G \frac{\partial w_a}{\partial z} = -\rho_p \frac{\partial M}{\partial t} - \varepsilon \rho_a \frac{\partial w_a}{\partial t} \quad (3.3)$$

Next a heat balance equation is derived for the system, relating to an overall change in enthalpy. If it is assumed that the heat applied to the system by the surrounding atmosphere is negligible, then it can be said that:

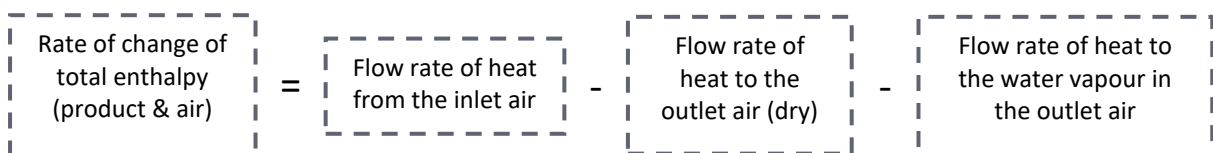


Figure 7: Heat balance guiding principle [23]

Lopez [23] goes on to further assume that the partial rate of change (with respect to time) in air temperature, air moisture content, and product temperature are all significantly close to zero, thereby arriving at the following equation:

$$\rho_p \frac{\partial M}{\partial t} [C_v(T_a - T_p) + L_p] = G(C_a + C_v w_a) \frac{\partial T_a}{\partial z} \quad (3.4)$$

A heat transfer rate equation must also be derived between the product and the drying air flowing through the layer. For given time interval (Δt), the following statement applies:

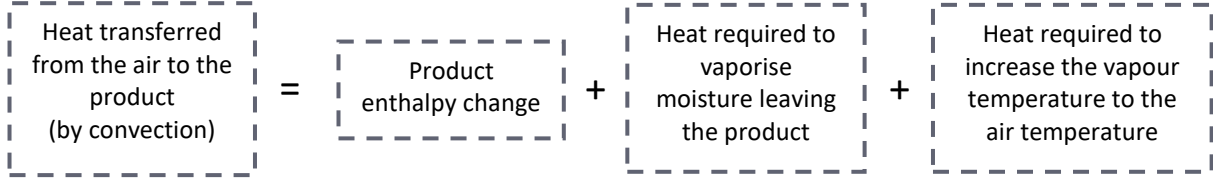


Figure 8: Heat transfer guiding principle [23]

After some light algebraic manipulation, the expression becomes [23]:

$$h_{cv}(T_a - T_p) = (C_p + C_w M) \frac{\partial T_p}{\partial t} - \frac{\partial M}{\partial t} (L_p + C_v T_a) \quad (3.5)$$

Where:

$$h_{cv} = h_c A_p \quad (3.6)$$

A drying rate equation is needed in order to describe the product's mass transfer rate. This is simply the thin-layer drying model for the produce and in the case of macadamia nuts, has already been derived by Palipane and Driscoll [18], and given in equation (3.1).

Then finite difference solutions must be derived for each of the above partial differential equations so that the system may be simulated and solved discretely. Keeping in mind the assumption made earlier, that the partial rate of change (with respect to time) of w_a is significantly close to zero, the finite difference solution to the moisture balance equation becomes [21, 23]:

$$\Delta w_a = -\rho_p \frac{\Delta z}{G} \left(\frac{\Delta M}{\Delta t} \right) \quad (3.7)$$

In order to find the finite difference solutions for equations (3.4) and (3.5) several further assumptions must be made. Lopez et al. [23] outline the following:

- No heat is lost or gained perpendicular to the flow of air through the bed;

- The heat lost or gained via conduction throughout the bed is negligible;
- Specific heats of water, water vapour and air remain constant; and
- The product's latent heat of vaporisation varies with its moisture content.

Using the mathematical model first described by Nellist [24], the finite difference solutions to the heat balance and heat transfer rate equations can be found. By equating the air's enthalpy change to that of the product and rearranging to find the change in air temperature, Lopez finds [21, 23]:

$$\Delta T_a = \frac{\frac{\rho_p \Delta Z}{G \Delta t} [\Delta M (C_v T_a + L_a - C_w T_p) - \Delta T_p (C_a + C_w (M + \Delta M))]}{C_a + C_v (w_a + \Delta w_a)} \quad (3.8)$$

For the heat transfer rate equation, Lopez equates the heat transferred between the air and product to the change in sensible heat of the product, plus the change in enthalpy of the water vapour after evaporating [23]. After rearranging to find changes in the product temperature, the finite difference solution becomes [21, 23]:

$$\Delta T_p = \frac{A + \rho_p \frac{\Delta M}{\Delta t} \left[\frac{2Y}{h_{cv}} + \frac{\Delta Z F}{GE} \right]}{1 + \frac{\rho_p}{\Delta t} \left[\frac{2B}{h_{cv}} + \frac{\Delta Z}{GE} (B + C_w \Delta M) \right]} \quad (3.9)$$

Where:

$$A = 2(T_a + T_p) \quad (3.10)$$

$$B = C_p + C_w M \quad (3.11)$$

$$E = C_a + C_v (w_a + \Delta w_a) \quad (3.12)$$

$$F = C_v T_a + L_a - C_w T_p \quad (3.13)$$

$$Y = L_p + C_v T_a - C_w T_p \quad (3.14)$$

Finally, some physical properties are required to solve the above system of equations. This includes [21, 23]:

- The product's specific heat capacity (C_p);
- The latent heat of desorption for the water contained within the product (L_p);
- The volumetric heat transfer coefficient by convection (h_{cv});

- The product's desorption isotherm used to calculate the equilibrium moisture content (M_e);
- Equations used to calculate the different conditions of humid air.
 - Moisture content (w_a),
 - Saturated vapour pressure (P_s),
 - Latent heat of water in air (L_a).

Using this model, it is possible to calculate the conditions of the outgoing wetted air travelling from one layer into the next. This is the crux of deriving a deep-bed model but is equally essential if using the thin-layer variant in its place; since the thin-layer model alone is not equipped to be validated against the available process data.

3.4 SIMULATION

Due to the prevalence of models for food drying processes, the associated simulations appear to also be quite abundant in literature. Following the model derivation for hazelnuts, Lopez et al. [21] provided the results of an associated discrete simulation. By using the finite difference forms of the aforementioned partial differential equations, the system could be simulated using the TurboBasic programming language and process reactions were analysed. A flow chart was given to describe how the simulation was programmed (Figure 9), and serves as a good foundation for how such a simulation might be replicated.

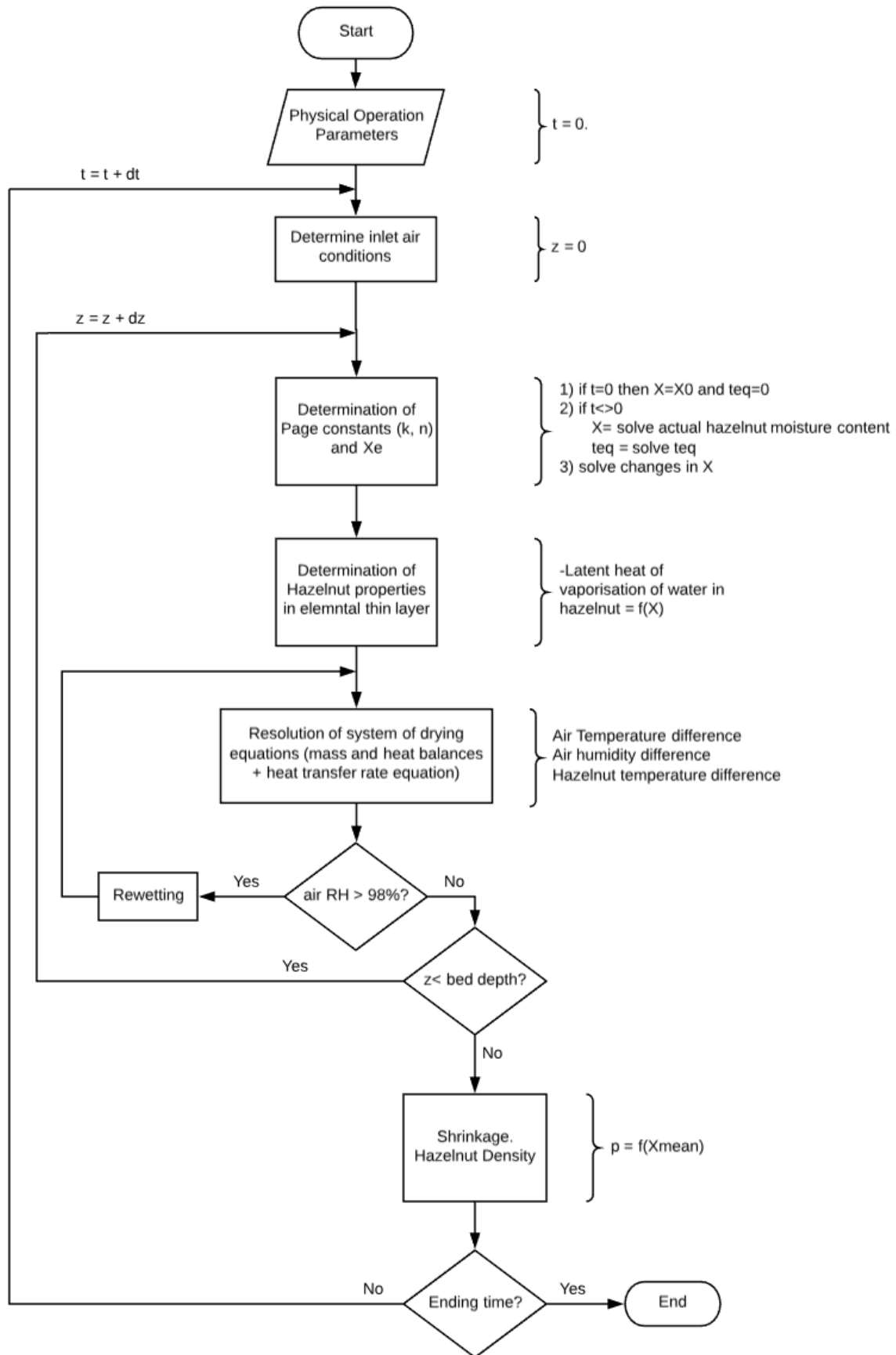


Figure 9: Logic flow chart for a discrete deep-bed hazelnut simulation [21]

Sitompul et al. produced a similar result for a deep-bed grain drying model [25] – a follow up publication to their comprehensive model derivation mentioned earlier [22]. Pankaew et al. [20] took a slightly different approach, creating a two-dimensional finite element simulation of the moisture transport within a single macadamia nut. This study gave an interesting insight into the moisture and temperature gradients that occur over the nut during drying [20], but is perhaps an excessive exercise for most engineering applications. Finally, Omid et al. [26] simulated the drying response of pistachio nuts using a multilayer feed-forward neural network (MFNN). The MFNN model consisted of 2 hidden layers with 8 and 5 nodes respectively, producing a higher grade of fitment to plant data than the 5 standard semi-empirical models considered [26]. Given recent advances in computational power, such a model has become increasingly viable. But the model itself provides no inference to the underlying transport process, given the abstract nature of a neural network. Thus, such a model makes the development of model-based controllers difficult, since the model developed takes on an incompatible form.

Chapter 4: CONTROL SYSTEM ARCHITECTURE

This chapter highlights what appears to be the largest gap in literature. Few publications have been issued which detail the specific control systems used to dry NIS macadamias. There could be several reasons for this, but it is suspected that techniques used in industry are either trivial or kept as trade secrets. Some mention is made toward various staged drying regimes [5, 14], but the specific detail of any feedback loops or control system architecture is absent for macadamias. The evidence within literature does however seem to suggest that the standard control philosophy of these processes is akin to an “expert system”, which tries to emulate decisions made by a human operator on a heuristic basis. Control system architecture is not a primary focus for this project. But given that the model and simulation is developed with control system design as its primary purpose, a brief review has been conducted nonetheless.

4.1 PROCESS CONTROL FOR FOOD DRYING

The number of process variables within a hot-air convective drying system is limited in comparison to some other process driven industries. The operator will ideally have control over the inlet air’s velocity, temperature and relative humidity in order to lower the average nut moisture content within the bed [15]. This can be achieved by manipulating the speed of the inlet fan, the rate of heat applied by an inlet heat exchanger, and the position of a damper – permitting the flow of recycled air. The main source of complexity in such a system arises with the challenge of drying quickly and efficiently, without causing degradation to product quality [13].

Szrednicki, Hou and Driscoll [27] developed a control system for the deep-bed drying of paddy. 5 different operating principles were tested, consisting of unique steady-state air flow, temperature and relative humidity targets. The architecture was quite simple, with PID controllers being implemented in a LabVIEW environment, interfacing with field instruments via a data acquisition card [27]. The

performance and economy of each scenario was reviewed, but no one scenario was given as an ideal operating principle.

Li, Ban and Shen [28] developed a self-adaptive control system for the drying of various grains. The scenario consisted of an expert system with a knowledge base of quality indicators, which allowed the program to make decisions toward suitable drying regimes based on traditional PID loops. Further to this, the controller included a model-based feed-forward control scheme to assist in counteracting disturbances and predicting the future effect of current control actions [28]. The system was tested on the drying of rice, with improvements to energy efficiency and product yield when compared to the legacy control scenario.

A rather complex example of a food drying control system can be found in the works of Lutfy et al. [29], where a simplified type-2 adaptive neuro-fuzzy inference system (ANFIS) was considered as a controller. The authors suggest that the proposed control system had a far superior performance when compared to the standard scenarios considered for the conveyor belt drying of grains [29]. However, the issue with such a scenario arises in its intricate nature, whereby an architecture which is easier to digest may be preferable in many agricultural applications. Although, artificial neural networks (ANN) have indeed been used in abundance within drying technology over recent years, both from a modelling and control perspective [30].

4.2 CONTROL STRATEGIES FOR MACADAMIA DRYING

When considering process control techniques suitable for macadamia drying, there are a few options. Conventional feedback control could be the most suitable for individual control loops, since the process is exceptionally slow and not subject to major disturbances and nonlinearities. Although, perhaps the system's simplicity warrants the use of more advanced control techniques, simply because they will not be too difficult to derive. The real complexity in such a task however, will likely

arise in building an “intelligent” system, which can update setpoints and drying regimes effectively, ensuring the quality of the product is maintained. Macadamias are quite susceptible to degradation, so any applied control system must be actively conscious of this. Rule based systems are perhaps the simplest to construct, but more complex scenarios encompassing aspects of optimisation and economics could be of greater value. More detail will be provided in Section 8.2 relating to future works, on how such a design task could be approached and successfully completed.

Chapter 5: VERIFYING THE LITERATURE

In order to develop a model and simulation based on resources found in literature, some preliminary actions must first be taken. The models, equations and theories presented by prior researchers must be validated and recreated before they can be built into a simulation for macadamias. By first recreating prior results, one can be sure that each component is understood, ready to be adapted for new purposes.

5.1 NIS MACADAMIA THIN-LAYER DRYING CHARACTERISTICS

Being that the thin-layer model plays such a pivotal role in any food drying simulation, this was first assessed. The thin-layer model presented by Palipane and Driscoll [18] was built into a MATLAB simulation, to ensure that this work could be recreated accurately. The work involved determining how a sample layer of nuts would dry under constant air velocity, temperature and relative humidity; providing the basis for more complex drying scenarios. Detailed descriptions of this work have been given in prior chapters, with this simulation primarily relying on equations (2.1) - (3.2). A logic flow diagram has been given in Figure 10 to help illustrate the program's structure.

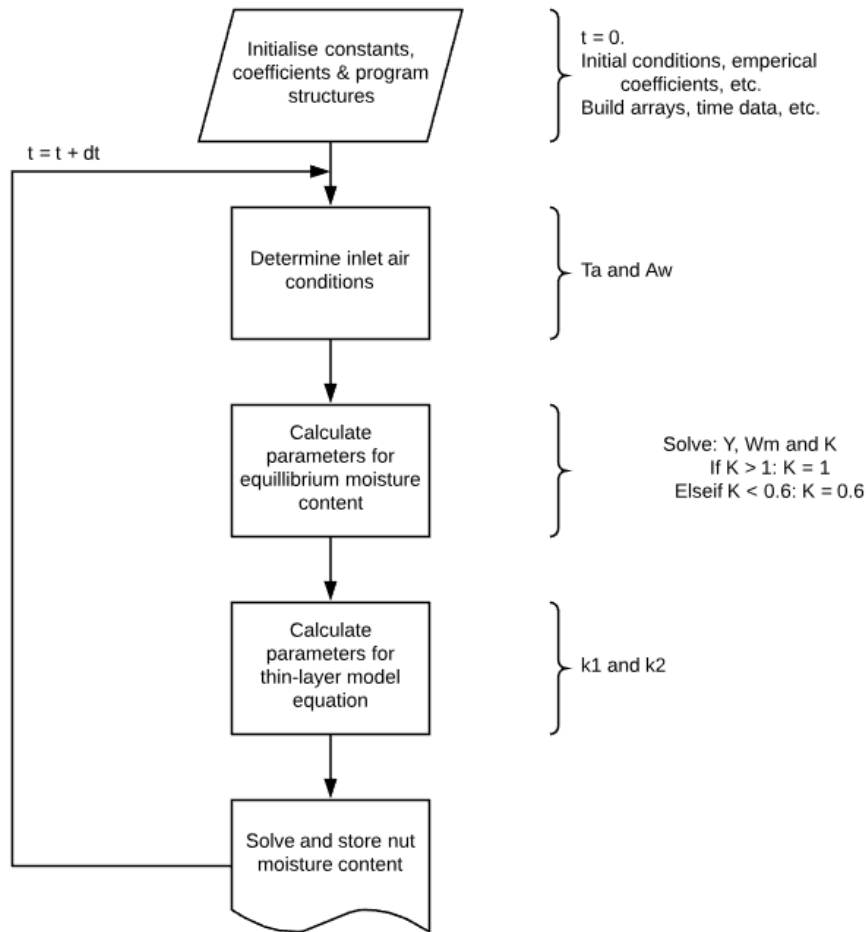


Figure 10: Logic flow diagram for thin-layer model verification

After running the simulation under the same test conditions used by Palipane and Driscoll, the responses shown in Figure 11 were obtained. The raw data used in the publication was unavailable, so a qualitative, visual assessment was used to verify that the results matched the literature. Figure 11 shows that the results obtained by the recreated simulation, which appear to closely match that of the original publication. The curious reader is encouraged to consult the original article by Palipane and Driscoll [18] to view a side-by-side comparison. The implication is that this research has been recreated successfully and is ready for adaptation into the forthcoming simulations. In addition to the result given in Figure 11, the recreated simulation provided a means to develop Figure 2 and Figure 3, assisting in the background discussion toward moisture sorption characteristics for macadamia nuts.

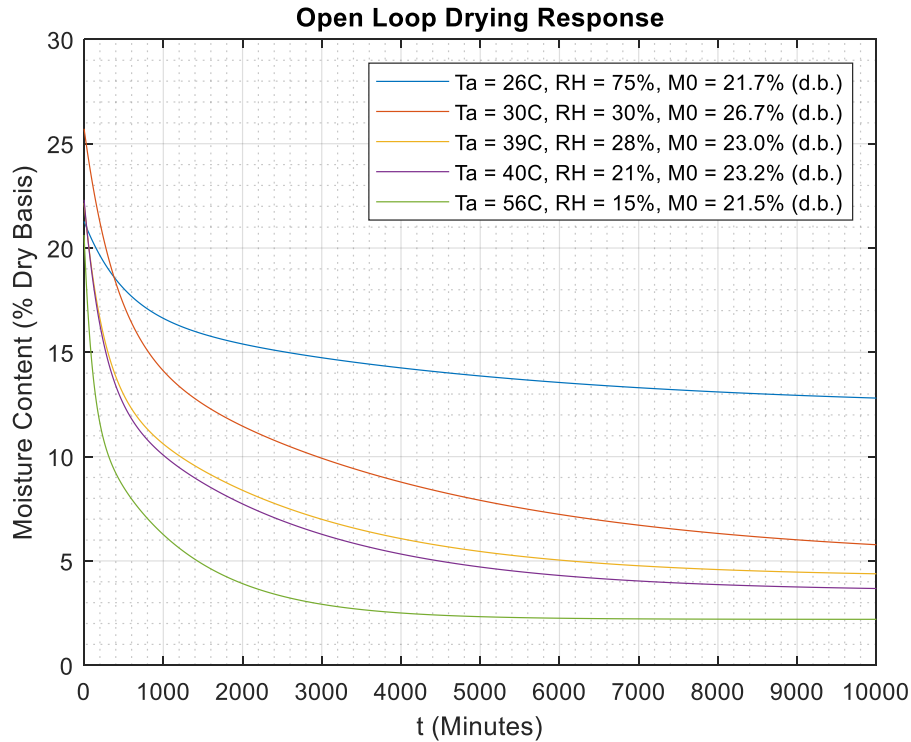


Figure 11: Verification of open loop response for thin-layer model

5.2 HAZELNUT DEEP-BED DRYING SIMULATION

The deep-bed algorithm developed in the works of Lopez et al [21, 23] remains a good starting point for such a model regarding macadamias. Hazelnuts and macadamias share some similarity in size and composition – both consisting of an outer shell and inner kernel – with industrial drying equipment for each being relatively identical. To ensure Lopez’s hazelnut drying simulation [21] is interpreted correctly, a replica of this simulation was constructed. There are several alterations to be made when undergoing an adaptation to macadamias, but conducting this validation ensures the concept is working prior to making any dramatic changes.

Verifying the work of Lopez proved to be far more challenging than that of Palipane and Driscoll. Aside from the scope being more complex, the over-simplification between steps, lack of explanation and some minor errors made it difficult to recreate this work. Nevertheless, this recreation was done successfully. To begin, Lopez gives the data in Table 1 to be used alongside the experiment [21].

Table 1: Data used for verification of the deep-bed algorithm [21]

Condition	Value
Initial hazelnut moisture content	20.62% (d.b.)
Initial hazelnut temperature	15°C
Diameter of hazelnut	0.016m
Bulk density	426 kg/m ³
Ambient air temperature	15°C
Ambient air relative humidity	75%
Drying air temperature	36°C
Drying air relative humidity	21.5%
Velocity of drying air	42.27 kg/min m ²
Bed cross sectional area	4.15 m ²
Bed depth	3.8 m
Drying time	12 h
Layer thickness	0.01 m
Specific heat of hazelnut	1.65 KJ/Kg

It is known that the specific heat of water and air are 4.19 KJ/Kg [31] and 1.005 KJ/Kg [32] respectively. The specific heat of water vapour in air varies over different temperatures, but is assumed constant at 1.87 KJ/Kg [33] given the limited temperature range considered. The thin-layer drying rate equation used is an approximation given by Page's equation (unlike the two-term exponential model used for macadamias), expressed as [21]:

$$\ln\left(\frac{M - M_e}{M_0 - M_e}\right) = -kt^n \quad (5.1)$$

Where:

$$k = 2.94 \exp\left(\frac{-1598}{273.15 + T_a}\right) \quad (5.2)$$

$$n = 0.5314 - 0.0014T_a - 0.0001RH \quad (5.3)$$

By differentiating with respect to time, and assuming M_0, M_e, k and n remain constant over a sufficiently small time interval, one can solve the associated finite difference equation as follows:

$$\frac{d \left[\ln \left(\frac{M - M_e}{M_0 - M_e} \right) \right]}{dt} = \frac{d[-kt^n]}{dt} \quad (5.4)$$

$$\frac{d[\ln(M - M_e) - \ln(M_0 - M_e)]}{dM} \frac{dM}{dt} = \frac{d[-kt^n]}{dt}$$

$$\frac{1}{M - M_e} \frac{dM}{dt} = -knt^{n-1}$$

$$\frac{dM}{dt} = -(M - M_e)knt^{n-1}$$

$$\Delta M = -(M - M_e)knt^{n-1}\Delta t \quad (5.5)$$

Interestingly, Lopez calculates the “equivalent” drying time for any given layer to dry to its current moisture content. This is to ensure that the drying rate of each layer is correct for the current moisture content, and not being modified collectively as time itself increases. The equivalent drying time for any position in the bed is given as [21]:

$$t_{eq} = \left[\frac{-\ln \left(\frac{M - M_e}{M_0 - M_e} \right)}{k} \right]^{1/n} \quad (5.6)$$

Thereby modifying equation (5.5) to become for any given layer [21]:

$$\Delta M = -(M - M_e)kn(t_{eq} + \Delta t)^{n-1}\Delta t \quad (5.7)$$

Finally, expressions are given for the:

- Latent heat of vaporisation of water in a hazelnut (L_p);
- Latent heat of vaporisation of water in air (L_a);
- Saturation vapour pressure of air (P_s); and
- Apparent moisture content of air (w_a).

$$L_p = L_a[1 + 0.5904\exp(-13.67M)] \quad (5.8)$$

$$L_a = 2500.6 - 2.3644T_a \quad (5.9)$$

$$P_s = \frac{\exp\left(14.293 - \frac{5291}{T_a + 273.15}\right)}{3.2917 - 0.01527(T_a + 273.15) + 2.54 * 10^{-5}(T_a + 273.15)^2} \quad (5.10)$$

$$w_a = 0.622 \frac{RHP_s}{P - P_s} \quad (5.11)$$

It should be noted that equation (5.10) given by Lopez to solve for P_s was found to be inaccurate. When validating the result of this equation against known values of the saturation vapour pressure of air, the result was found to be off by a factor of 10^5 . To avoid the inclusion of any corrective coefficients which have no underpinning scientific basis, an alternative equation for P_s was found in literature and used in its place [34]:

$$P_s = \frac{C_1}{T_a} + C_2 + C_3T_a + C_4T_a^2 + C_5T_a^3 + C_6 \ln(T_a) \quad (5.12)$$

Where:

$$\begin{aligned} C_1 &= -5800.2206 & C_2 &= 1.3904993 \\ C_3 &= -0.04860239 & C_4 &= 0.41764768 * 10^{-4} \\ C_5 &= -0.14452093 * 10^{-7} & C_6 &= 6.5459673 \end{aligned}$$

This assembles all the necessary components to generate a discrete simulation for the deep-bed drying of hazelnuts, alongside the finite difference equations given earlier in equations (3.7) - (3.9). This program attempts to follow a similar structure to that described in the works of Lopez [21] in Figure 9.

Figure 12 serves as a comparison to Lopez's breakdown of changes in nut moisture content across layers in the bed during drying [21]. The two simulations are nearly identical, with the bottom layer reaching about 5% (d.b.) moisture content after 12 hours of drying, and succeeding layers lagging as

expected. The comparison verifies that the simulation is working correctly, as per the original publication.

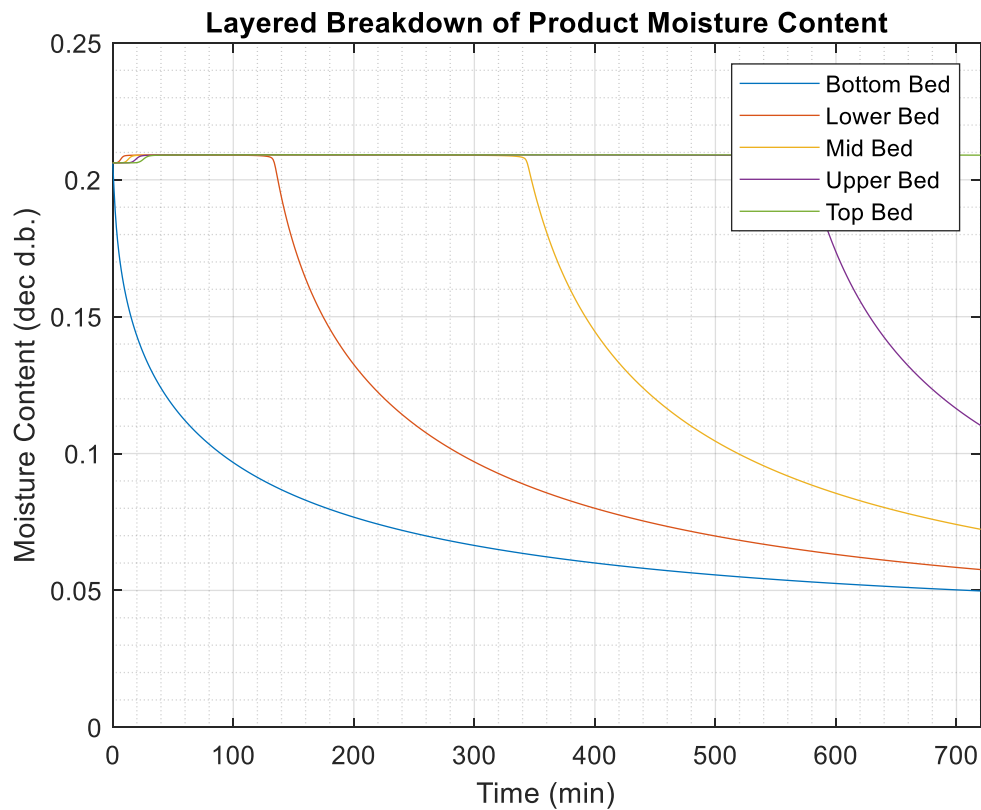


Figure 12: Verification of changes in product moisture content for deep-bed simulations

Interesting to note however, is the additional information attainable by the higher resolution results given in Figure 12. The moisture content throughout the bed reaches a new, higher steady state once drying is commenced. This is due to moisture being extracted from lower regions and rewetting subsequent layers until enough moisture has been extracted below to then begin drying the higher regions. This affect is more pronounced for a higher drying air humidity. Additionally, the increased resolution shows that the initial drying period of each layer is less sigmoidal than Lopez's figure suggests.

Chapter 6: MODEL CONSTRUCTION

Now that the individual components necessary to build a deep-bed model are understood, this may be adapted to suit a simulation for macadamias. There are various alterations that must be made to the algorithm before it will function correctly. What was first assumed to be simple plug-and-play task, has since proven to be more challenging in execution. This chapter highlights the key steps taken to adjust the algorithm to suit the purpose of this study.

6.1 DESIGN, LAYOUT AND STRUCTURE

Up to this point, the primary focus has been on the process of drying the produce specifically, with little consideration given to components beyond this boundary. So far, the system's inputs have been considered to be the inlet air velocity, temperature and relative humidity, whilst its outputs have been attributed to nut moisture content, and the outlet air conditions. This of course is not entirely practical, since the inlet air conditions are not directly manipulable. Instead, the available manipulated variables (MVs) include:

- The heat exchanger's flow control valve, regulating the flow of a heating medium which affects the inlet air's temperature;
- The inlet air damper, regulating the mixture of ambient and recycled air streams for the inlet air; and
- The signal sent to the inlet fan's variable speed drive (VSD), regulating the flow rate of drying air through the system.

If any successful control system is to be implemented, then additional relationships must be found to describe how the MVs affect the inlet air conditions. However, the inlet air conditions are not only affected by the MVs, but also any disturbances and recycle streams that exist within the process. Thankfully, the system being studied here has the ability to measure some of these disturbances and

can thereby account for them in the model. Figure 13 consists of a block diagram which details how these individual processes are interconnected, building the overall open-loop model structure. Each process is illustrated as a “black box” for now, with very little inferred about the underlying process characteristics.

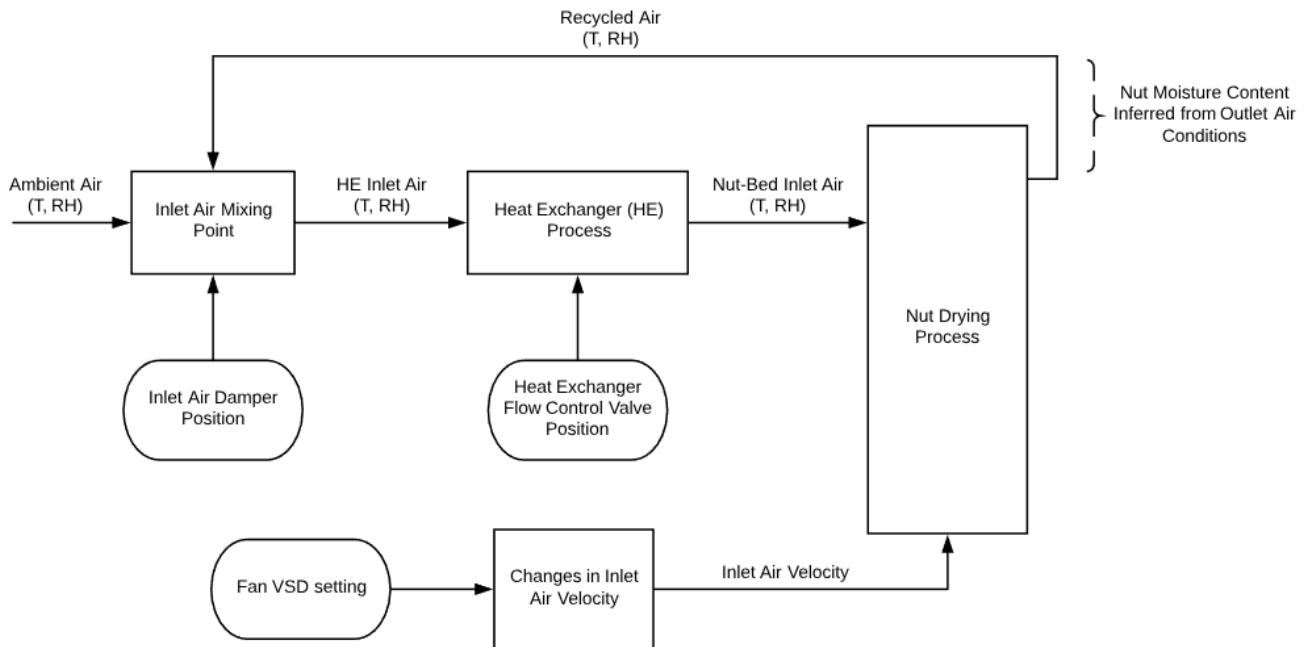


Figure 13: Overall open-loop process block diagram

The “nut drying process” is simply the deep-bed model and has already been discussed extensively in prior chapters. To formulate models for the subsidiary processes shown in Figure 13, a combination of empirical and theoretical modelling techniques will be used. A decision was made to not model the changes in inlet air velocity. As mentioned in Section 3.2 the influence of inlet air velocity on drying dynamics is of a much smaller magnitude than the air temperature and relative humidity. This simplification allows for a better focus on process variables which do indeed have a noticeable effect on process dynamics. Thus, inlet air velocity will remain constant for the purpose of this simulation, despite being variable in nature. This property may still be stepped to view its open-loop response, but no relationship to the fan VSD setting has been developed. Perhaps in future studies this may be included as an extra degree of accuracy, but for the purpose of this project it has been deemed negligible.

6.2 SUBSIDIARY PROCESS MODELS

It is at this time necessary to outline how the subsidiary processes shown in Figure 13 are constructed. The purpose of this section is to better define these model structures, and clearly outline the underlying mechanics of each. With regard to deriving the heat exchanger's model specifically (given in Section 6.2.2), there are some concepts which are perhaps too exhaustive for the purpose of this chapter – yet still require an explanation. Such omissions will be noted wherever necessary, with a redirection given to the reader as to where this information can be found elsewhere in this document.

6.2.1 Inlet Air Mixing Process

The initial mixing point which exists prior to both the inlet fan and heat exchanger is considered to be subject to the following initial assumptions:

- There exists no mass hold-up at the mixing point;
- The volumetric flowrate of the outlet is equal to the sum of the two inlet volumetric flowrates, and thus the air pressure before and after the mixing point is equivalent;
- This constant air pressure is equal to that of the inlet air pressure at the bottom of the nut-bed;
- The temperature and relative humidity of the recycle stream is equal to that measured at the top of the nut-bed;
- The outlet of the mixing point is a well-mixed product of the two inlet streams;
- The inlet damper's position correlates to a linear mix of the two incoming air streams;
- A damper position of 100% implies an inlet composing entirely of ambient air, whilst 0% suggests entirely recycled air;

The last assumption given above can be further verified when considering that the pressure drop which exists on either side of the inlet fan will always be equal. Thus, assuming that both the inlet and exhaust points on the apparatus both have the same cross sectional area, the air will not recirculate

when the damper is open, and entirely recirculate when the damper is closed. Figure 15 is given to better illustrate this comparison.

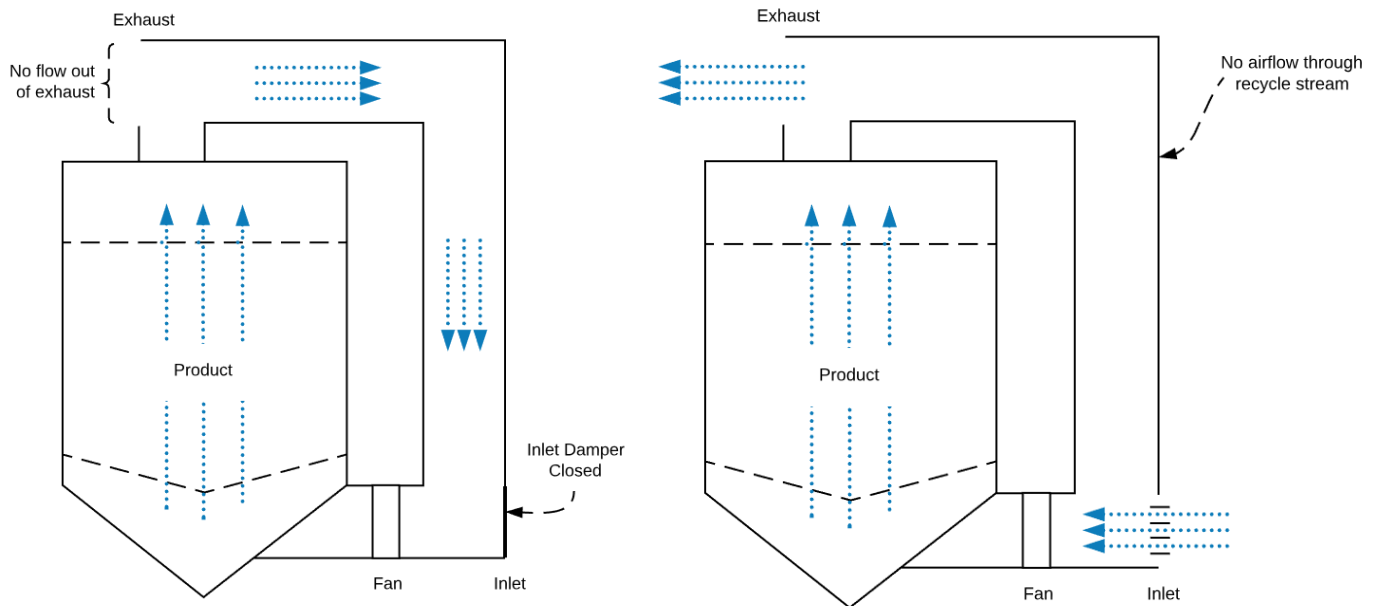


Figure 15: Comparison of airflow for fully open and fully closed inlet damper positions

These assumptions make it easier to model the inlet mixing point, without deviating too far from the actual process dynamics. This results in a straight-forward mixing problem, illustrated by Figure 14.

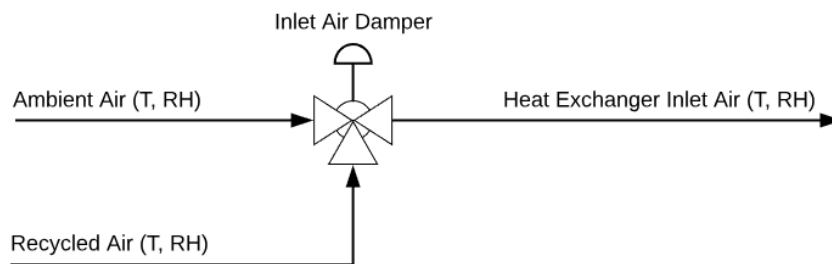


Figure 14: Diagram of the inlet air mixing point

However, this mixing problem is unique in that it requires consideration toward the psychrometric properties of moist air. Air is able to hold different quantities of moisture at different temperatures; hence the term “relative” humidity, since the air’s capacity to hold moisture is relative to its temperature. Air which is heated will see a decrease in its relative humidity, despite maintaining the same mass fraction of water vapour [34, 35]. Thus for the mixing problem given in Figure 14, the resulting temperature and relative humidity of the outlet air must be found from two independent

streams of moist air. The temperature of the outlet stream is simply found by rearranging the following component balance [35]:

$$T_f(\dot{V}_A + \dot{V}_R) = \dot{V}_A T_A + \dot{V}_R T_R \quad (6.1)$$

If D is considered to be the decimal form of the inlet damper's position, then the prior assumption that the damper linearly mixes the two streams of air (which are of equal pressure and density) implies that:

$$T_f(D + 1 - D) = D T_A + (1 - D) T_R \quad (6.2)$$

$$T_f = D T_A + (1 - D) T_R \quad (6.3)$$

Solving for the outlet stream's relative humidity is more complicated, with the same linear mixing equation not being directly applicable. Instead, the moisture content of each air stream must be calculated as a mass fraction, and then the same balance equation may be applied. This mass fraction is called the "humidity ratio" (W) and is defined as the ratio of water vapour to dry air:

$$W = \frac{M_w}{M_a} \quad (6.4)$$

Bullock and Geer [34] provide some useful arrangements of fundamental psychrometric equations which can be used to solve the different properties of moist air. It is stated that the humidity ratio may also be calculated as [34]:

$$W = 0.62198 \frac{P_w}{P - P_w} \quad (6.5)$$

Where P_w is the partial pressure of water vapour, calculated from the product of relative humidity the air and the saturation pressure of water vapour (P_s) [34]:

$$P_w = RHP_s \quad (6.6)$$

Where P_s is a function of air temperature and given in equation (5.12). Once the humidity ratios of both inlet streams are known, then the following component balance applies [35]:

$$W_f(\dot{V}_A + \dot{V}_R) = \dot{V}_A W_A + \dot{V}_R W_R \quad (6.7)$$

$$W_f(D + 1 - D) = DW_A + (1 - D)W_R \quad (6.8)$$

$$W_f = DW_A + (1 - D)W_R \quad (6.9)$$

Which is essentially the same linear mix used to solve the outlet air temperature. Finally, the outlet air's relative humidity is calculated by rearranging equations (6.5) and (6.6) to find:

$$P_w = \frac{WP}{0.62198 + W} \quad (6.10)$$

$$RH = \frac{P_w}{P_s} \quad (6.11)$$

Thus providing all the equations needed to define the inlet air mixing process.

6.2.2 Inlet Air Heat Exchanger Process

This model was not derived from first principles, unlike what has been done for other sections of the plant. Instead, an empirical approach was used, given the lack of information known about the heat exchanger, the flowrate of air through it and the operating conditions of its heating medium. This was an iterative task, with many different model structures considered. The structures investigated included various input and output configurations, attempting to find a form which was readily adaptable for the simulation, whilst still remaining accurate. Some of the failed model structures included those given in Table 2.

Table 2: Failed heat exchanger empirical model structures

Configuration	Inputs	Outputs
4 inputs, 2 Outputs	Ambient T, Ambient RH, Recycle T and Recycle RH	Outlet T, Outlet RH
4 Inputs, 1 Output	Ambient T, Recycle T, Damper Position, Valve Position	Outlet T
4 Inputs, 1 Output	Ambient RH, Recycle RH, Damper Position, Valve Position	Outlet RH
3 Inputs, 2 Outputs	Inlet T, Inlet RH, Valve Position	Outlet T, Outlet RH

Each configuration was tested for validity using MATLAB’s system identification toolbox to test different model forms. The types of models tested in the system identification toolbox included: transfer function models, state space models and non-linear autoregressive with exogenous terms (ARX) models. The most applicable model structure of those considered was found to be the most simple; being a linear, single input, single output (SISO) approximation with one disturbance. In truth, the actual process dynamics are non-linear and hence more complicated than those suggested here, but the approximation appears to perform adequately for the purposes of this simulation. For this approximation, the heating medium’s flow control valve is the input, the heat exchanger’s outlet air temperature is the output, and the inlet air temperature (resulting from the previously discussed mixing point) is the disturbance. Figure 16 gives a simplified process block diagram of how this process is arranged.

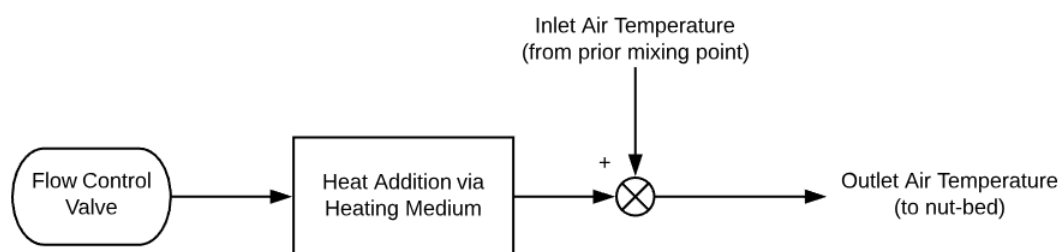


Figure 16: Heat exchanger approximated model structure

There are a few fundamental flaws with this model structure. Firstly, the inlet air temperature is actually an input disturbance (not an output disturbance) and thus, incorrectly represented in this approximation. Additionally, the approximation assumes that any given valve position correlates to a commensurate steady-state addition to outlet temperature. This is of course not correct since this should be dependent on the difference in temperature between the inlet air and the heating medium. However, given the lack of measurable process information on this sub-system, concessions must be given.

Before the approximate model could be empirically found using MATLAB's system identification toolbox, the plant data had to be "cleaned". This includes:

- Removal of duplicate and redundant data points;
- Homogenising the time step between data points to artificially create a regularly sampled dataset.
 - This was done by either interpolating between neighbouring data points or applying a zero-order-hold (depending on the variable).
- Filtering of certain variables to reduce noise and high frequency movements, which otherwise make it difficult for MATLAB to iterate toward an approximate model.

A more detailed discussion into each of these techniques, their importance and how they are executed is given in Section 7.1. It is not the intention of this chapter to overburden the reader with the specific details toward MATLAB coding and simulation design; such topics are better suited to the forthcoming discussion regarding the integration of plant data and model verification. The empirical model found to provide the most accurate approximation whilst remaining sufficiently simple to implement is given in equation (6.12).

$$T_{out}(s) = \frac{11.679(1.0637 * 10^5 s + 1)}{(1.01 * 10^5 s + 1)(4911.9 s + 1)} U_{HE}(s) + T_f(s) \quad (6.12)$$

Where U_{HE} is the heat exchanger's valve position. The reader is encouraged to consult Appendix B for a step-by-step walkthrough of how this approximate model is obtained using MATLAB's system identification toolbox. Now that both the inlet mixing point and heat exchanger have been modelled, the focus may be shifted to the development of a drying simulation for NIS macadamias.

6.3 SIMULATION DEVELOPMENT

At first it was expected that building a drying simulation for macadamias would simply involve piecing together the different model components. However, in practice this is not the case. Given the mathematical differences in the macadamia's thin layer model, and differences in their drying characteristics to hazelnuts, there were additional difficulties.

6.3.1 Constructing the Deep-Bed Simulation

The deep-bed model developed for hazelnuts was modified to include the relevant physical properties of macadamia nuts, and the details of the specific systems to be simulated. This included quantities such as physical dimensions, specific heat capacities, empirical coefficients and the like. This of course plays a role in updating crucial model components (like desorption isotherms for example), so they accurately represent the dynamics of macadamia nuts. Following this, the thin-layer model for macadamias had to be incorporated into the simulation. Some superficial changes were made from the outset, namely due to:

- Palipane and Driscoll's thin-layer drying equation [18] was originally designed with time in minutes, whilst Lopez's simulations [21, 23] rely on time being in seconds;
- Palipane and Driscoll express moisture content as a percentage [18], whilst Lopez uses the decimal equivalent [21];
- Inconsistencies occurred throughout with temperature being expressed as either Kelvin or Celsius;

- Various scaling errors were found throughout the work of Lopez [21], where dimensional analysis revealed that some quantities had been allocated the wrong units.

Next, the finite difference form of the thin-layer model must be solved to find ΔM , much like that which has been shown in the derivations from equation (5.4) to equation (5.5). The thin-layer drying equation was given earlier in equation (3.1) and is expressed as [18]:

$$\frac{M - M_e}{M_0 - M_e} = c_1 \exp(-k_1 t) + c_2 \exp(-k_2 t) \quad (3.1)$$

Following the same operations as those performed on equation (5.4) assuming M_0, M_e, c_1, c_2, k_1 and k_2 remain constant over a sufficiently small time interval, the discrete change in product moisture content can be found:

$$\frac{d \left[\frac{M - M_e}{M_0 - M_e} \right]}{dt} = \frac{d[c_1 \exp(-k_1 t) + c_2 \exp(-k_2 t)]}{dt} \quad (6.13)$$

$$\frac{1}{M_0 - M_e} \left[\frac{dM}{dt} - 0 \right] = -k_1 c_1 \exp(-k_1 t) - k_2 c_2 \exp(-k_2 t)$$

$$\frac{dM}{dt} = -(M_0 - M_e)[k_1 c_1 \exp(-k_1 t) + k_2 c_2 \exp(-k_2 t)]$$

$$\Delta M = -\Delta t(M_0 - M_e)[k_1 c_1 \exp(-k_1 t) + k_2 c_2 \exp(-k_2 t)] \quad (6.14)$$

At this point, it would be ideal to solve for the equivalent drying time like that shown previously in equation (5.6). But this is not possible, given that the variable t exists in the exponent of a sum of two exponential Euler terms. No general solution for such an equation exists [36], with mathematicians relying on either numerical methods or a Taylor series expansion to approximate the solution.

The Taylor series method was first attempted with inaccurate results for low-order approximations, and the resulting polynomial equation become quite difficult to solve for high-order approximations.

The numerical method was far more applicable to this scenario, given the computational nature of

the simulation. The MATLAB function `fzero()` was deployed, which tries to find the zero of a function by numerically adjusting a given variable. This worked well for purely simulated test runs, but would consistently crash the program when conducting later attempts at model validation using real plant data. The reason for this is still unknown, but a workaround was developed nonetheless – detailed in Appendix C. The workaround given in Appendix C is somewhat crude in comparison to the `fzero()` method, but gives acceptable results under validation.

The latent heat of water in the product was updated to reflect the experiments conducted by Palipane and Driscoll [11], since this too differs from that of hazelnuts:

$$L_p = L_a [1 + 1.074 \exp(-0.266 M_{\%})] \quad (6.15)$$

Without delving too far into the “computer science” aspect of such a programming task, this concludes the primary modifications made to the deep-bed simulation in order to suit NIS macadamias.

6.3.2 Implementing Subsidiary Processes

The only activity remaining in order to construct the open-loop simulation, is to implement the subsidiary processes developed in Section 6.2. In the case of the inlet air mixing point, this is relatively simple. There is no complex dynamics to consider here, so simply implementing the necessary equations into a subroutine is sufficient. A MATLAB function “`AirMixing()`” was developed which requires the input of temperature and relative humidity data for both recycle and ambient streams, as well as the inlet dampers position reading. For each time-step, the function solves the resulting temperature and relative humidity of the mixing outlet using equations (6.3), (6.5), (6.6) and (6.9) - (6.11).

The heat exchanger’s approximate model was transformed into a suitable form for a discrete simulation. The z-transform of the transfer function contained in equation (6.12) was found for a 60 second sample time, and then converted into a difference equation:

$$G_{HE}(s) = \frac{11.679(1.0637 * 10^5 s + 1)}{(1.01 * 10^5 s + 1)(4911.9s + 1)} \quad (6.16)$$

$$G_{HE}(z) = \frac{Az^{-1} - Bz^{-2}}{1 - Cz^{-1} + Dz^{-2}} \quad (6.17)$$

$$Y_{HE}(k) = CY_{HE}(k - 1) - DY_{HE}(k - 2) + AU_{HE}(k - 1) - BU_{HE}(k - 2) \quad (6.18)$$

Where:

$$A = 0.1502452521578261$$

$$B = 0.1501605034962723$$

$$C = 1.98719083254125$$

$$D = 0.9871980890410829$$

At first glance, these coefficients appear to have an unnecessary degree of precision, with many decimal places which could have perhaps been rounded off. However, such rounding results in dramatic changes to the pulse transfer function, causing it to behave in a vastly unexpected manner. In fact, when using MATLAB's `c2d()` function, and taking the calculated coefficients from the z-domain into a difference equation, the observed step response is unreasonably deviant from the expected output. Figure 17 shows the magnitude of this discrepancy, and just how poor the explicit `c2d()` result performs within a difference equation. It is suspected that due to the very large time constants in the continuous transfer function, the reliance on accurate decimal places in the pulse transfer function is magnified.

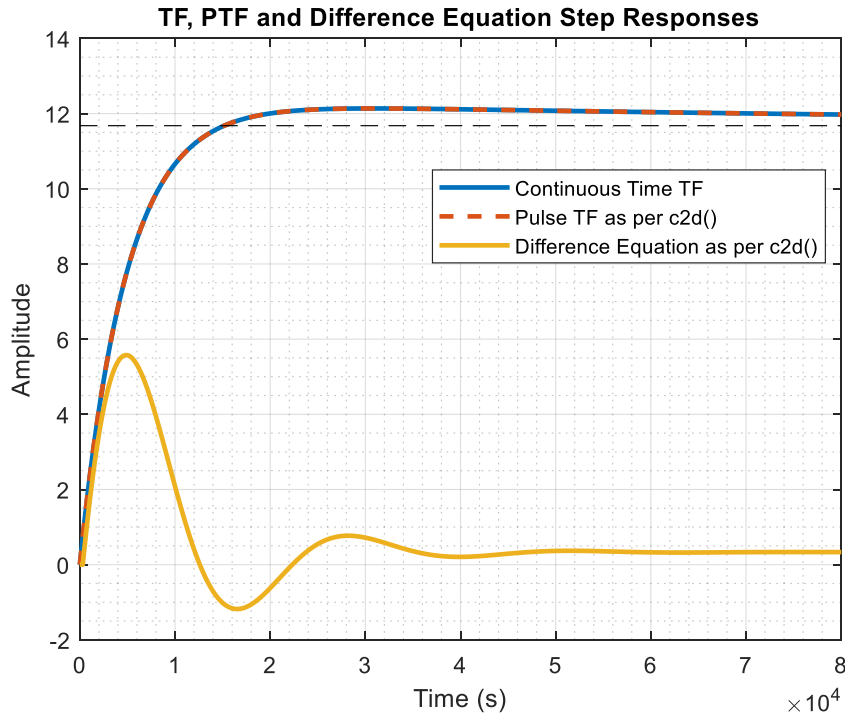


Figure 17: Step response of continuous, discrete and difference model variants

It should be noted that the pulse transfer function obtained by `c2d()` used without conversion into the k -domain, does perform as expected. This suggests that the coefficients “underneath the hood” do indeed maintain a high level of precision, but those output to the command window to be read by the user have been rounded. The MATLAB command “`>> format LongE`” will allow the display of numbers at higher levels of precision in the command window, but this is not compatible with `c2d()`. No equivalent method is known by the author for displaying a higher precision output from the `c2d()` function.

Since the explicit output from `c2d()` was deemed unreliable, the coefficients A, B, C and D were found in a more analytical, round-about way. The inverse Laplace transform of equation (6.16) was found in order to bring the equation into the time domain, then the difference equation was developed from that result. The coefficients A, B, C and D are by this means solved algebraically:

$$G_{HE}(s) = \frac{K_p(\tau_z s + 1)}{(\tau_{p1} s + 1)(\tau_{p2} s + 1)} \quad (6.19)$$

$$[\tau_{p1}\tau_{p2}s^2 + (\tau_{p1} + \tau_{p2})s + 1]Y_{HE}(s) = K_p(\tau_z s + 1)U_{HE}(s) \quad (6.20)$$

$$\tau_{p1}\tau_{p2} \frac{d^2 y_{HE}}{dt^2} + (\tau_{p1} + \tau_{p2}) \frac{dy_{HE}}{dt} + y_{HE}(t) = K_p \left[\tau_z \frac{du_{HE}}{dt} + u_{HE}(t) \right] \quad (6.21)$$

$$\begin{aligned} \tau_{p1}\tau_{p2} \frac{y_{HE}(k+2) - 2y_{HE}(k+1) + y_{HE}(k)}{\Delta t^2} + (\tau_{p1} + \tau_{p2}) \frac{y_{HE}(k+1) - y_{HE}(k)}{\Delta t} \\ + y_{HE}(k) = K_p \left[\tau_z \frac{u_{HE}(k+1) - u_{HE}(k)}{\Delta t} + u_{HE}(k) \right] \end{aligned} \quad (6.22)$$

$$Y_{HE}(k) = CY_{HE}(k-1) - DY_{HE}(k-2) + AU_{HE}(k-1) - BU_{HE}(k-2) \quad (6.23)$$

Where:

$$A = \frac{K_p \tau_z \Delta t}{\tau_{p1} \tau_{p2}} \quad (6.24)$$

$$B = \frac{-K_p \Delta t (\Delta t - \tau_z)}{\tau_{p1} \tau_{p2}} \quad (6.25)$$

$$C = \frac{-\Delta t (\tau_{p1} + \tau_{p2}) + 2\tau_{p1} \tau_{p2}}{\tau_{p1} \tau_{p2}} \quad (6.26)$$

$$D = \frac{-\Delta t^2 + \Delta t (\tau_{p1} + \tau_{p2}) - \tau_{p1} \tau_{p2}}{\tau_{p1} \tau_{p2}} \quad (6.27)$$

Thus, when solved using the approximate model's design parameters, the coefficients given in equation (6.18) are found. As shown in Figure 18, the analytically derived difference equation performs accurately unlike that adapted from the c2d() function in MATLAB.

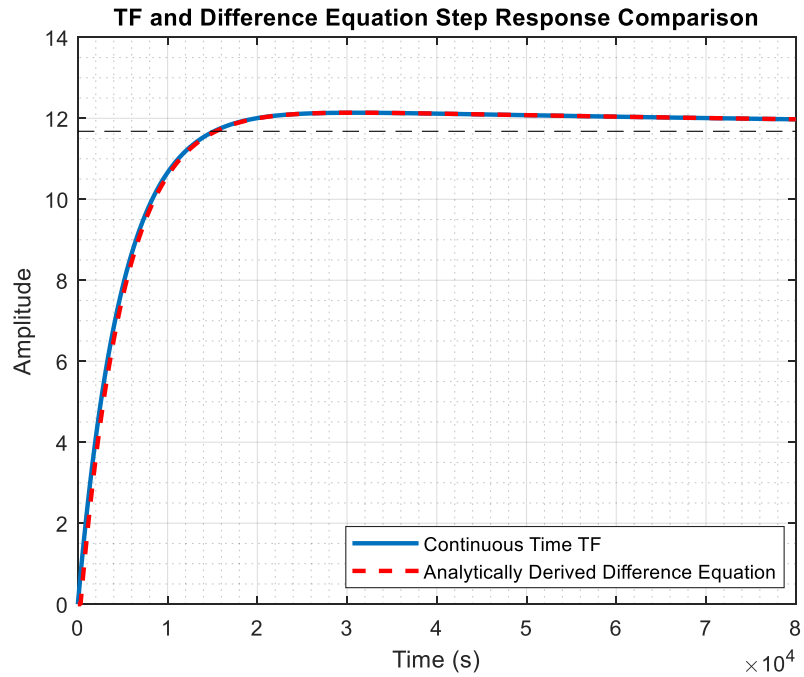


Figure 18: Comparison of an analytically derived difference equation to its continuous time transfer function for the heat exchanger approximate model

6.3.3 Finalised Open-Loop Simulation

Now that the open-loop simulation has been constructed in its entirety, it is possible to view its output and monitor process reactions to different input steps. Figure 19 provides a logic flow diagram outlining the final structure of the open-loop simulation.

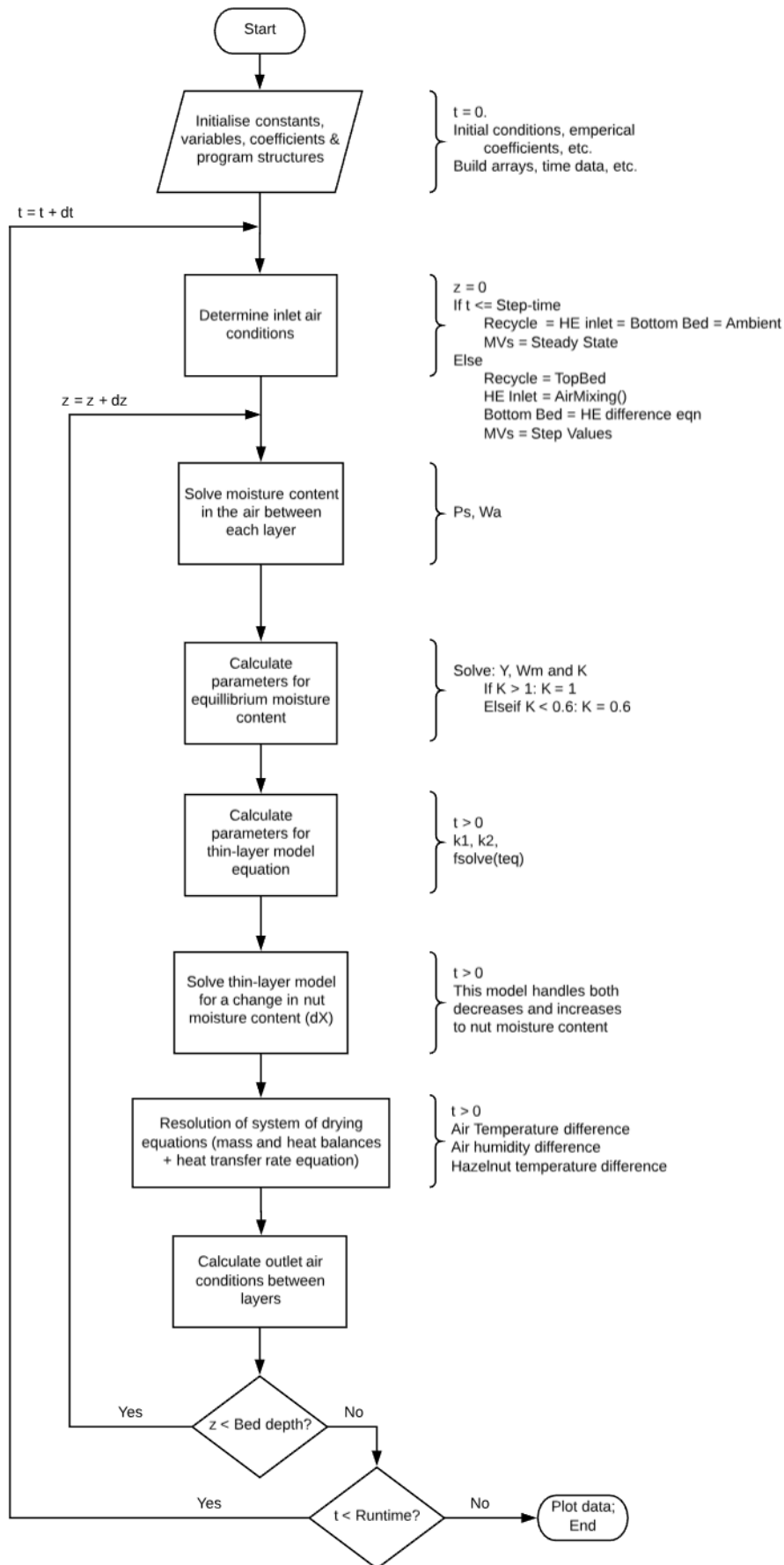


Figure 19: Logic flow diagram for open-loop simulation

To begin, process reactions for a simple drying scenario are monitored, with no steps to manipulated variables, implying constant inlet air conditions. All simulated drying runs will assume the system parameters given in Table 3.

Table 3: Constant system parameters for simulation

Property	Constant Value
Nut-Bed Depth	2.5m
Silo Inner Diameter	4.2m
Nut-Bed Inlet Pressure	102KPa (Absolute)
Mass Flowrate of Drying Air	0.4Kg/s
Elementary Layer Thickness	0.5m
Discrete Sample Time	60s

For a drying run with no MV steps, no recycled air and the initial conditions given in Table 4, the responses exhibited by Figure 20 are found.

Table 4: Open-loop simulation - process parameters

Property	Initial Condition
Nut Moisture Content	21% (W.B.)
Product Temperature	25°C
Ambient Temperature	25°C
Ambient Relative Humidity	30%
Inlet Damper Position	100%
Inlet Heater Valve Position	0%

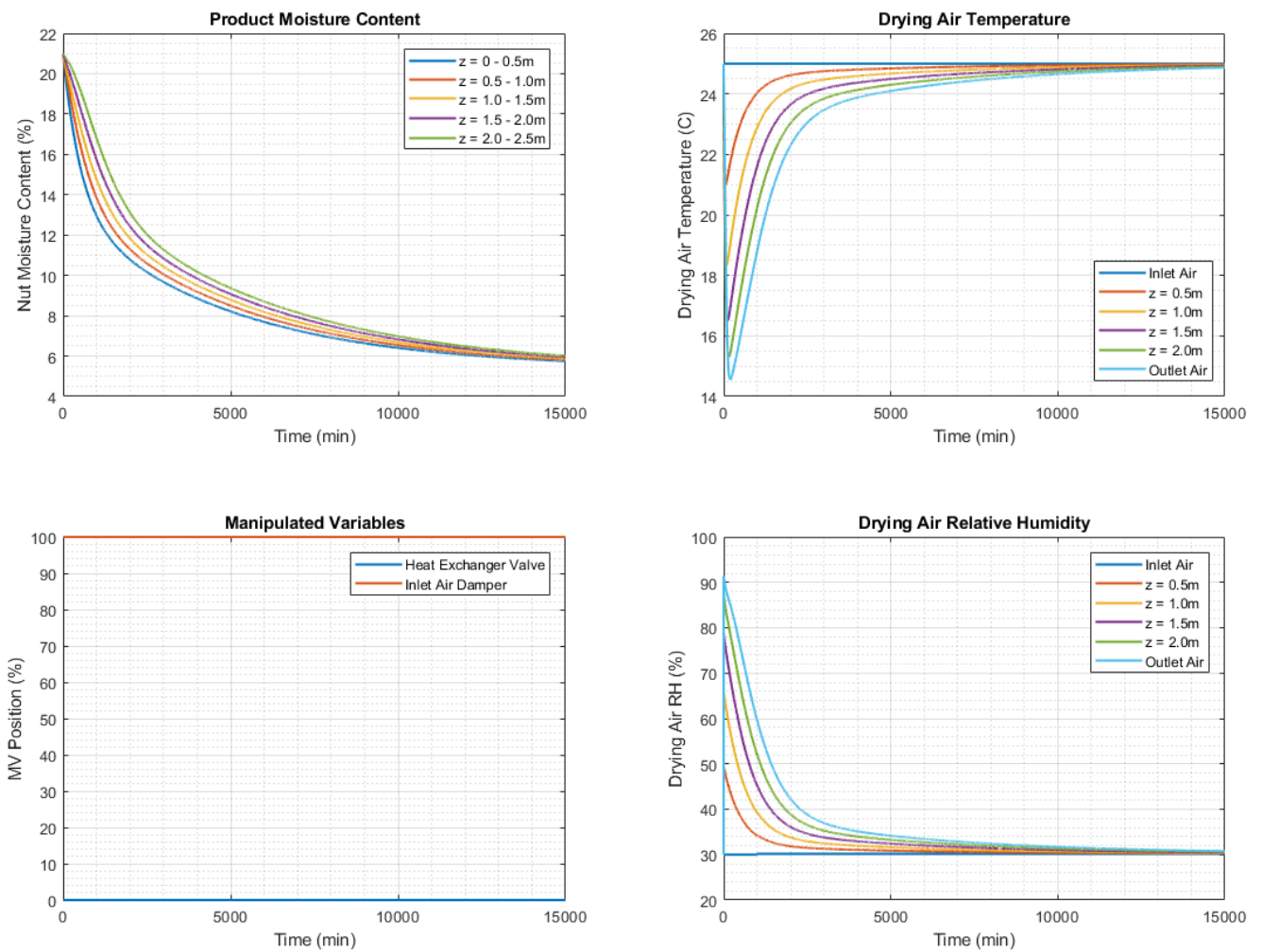


Figure 20: Open-loop simulation #1 - process reactions

The process reactions observed in Figure 20 coincide with what should be expected from a physical system. A “drying front” can be observed moving through the nut-bed on both the nut moisture content and drying air conditions, such that lower regions see a faster decrease in moisture. The nut-bed itself behaves in a way similar to that of a second heat exchanger, cooling the drying air as it passes the wet product. Upper layers also experience a higher relative humidity as the moisture from lower regions is passed through to subsequent layers in the bed. All of these effects slowly decrease in magnitude as the product approaches its equilibrium moisture content, which in this case appears to be between 5-6% (W.B.). The drying run extends for 15000 minutes, or approximately 10 days, a reasonable drying time for no heat addition or recycling of the drying air. It should be noted that in

reality, the ambient air conditions would fluctuate over the 10 day period – a fact that is not yet considered in these preliminary simulations.

The effects of both the inlet air damper and heat exchanger can also be examined by individually stepping either manipulated variable. Under the same initial conditions as the prior simulation given in Table 4, the effect of stepping the inlet damper from a position of 100% to 50% at $t = 1000$ minutes is observed in Figure 21.

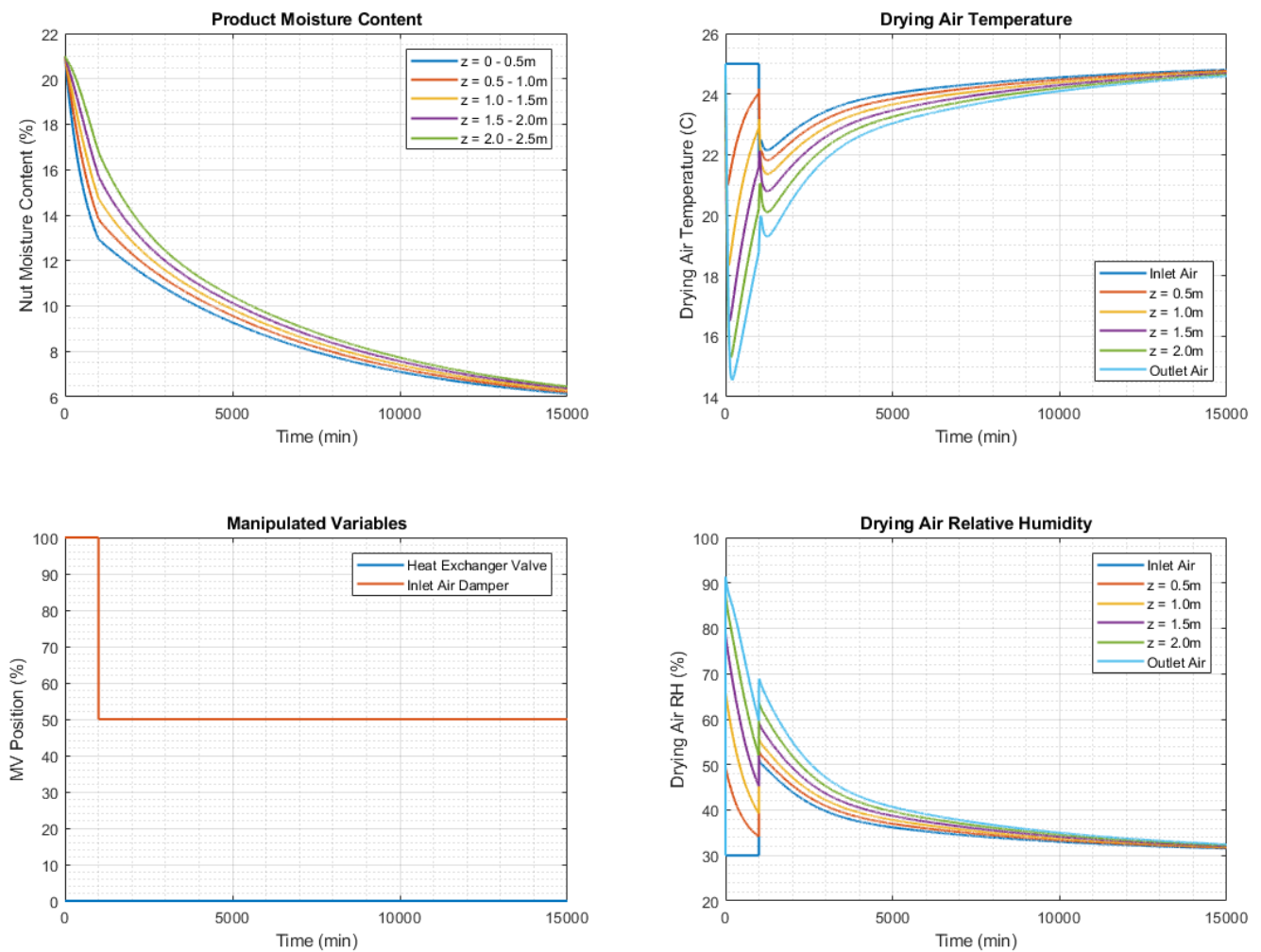


Figure 21: Open-loop simulation #2 - process reactions

Again, the simulation performs as one would expect. The cool, wetted air which has passed through the nut-bed is being recycled at a rate of 50% with the warmer ambient air. This has slowed the rate of drying when compared to the previous simulation and caused a noticeable jump to the drying air conditions. Finally, a likewise observation can be made toward the effect of the inlet heat exchanger

under the same initial process conditions given in Table 1. Figure 22 exhibits the process reaction after a step to the heat exchanger's valve position from 0% to 50% at $t = 1000$ minutes.

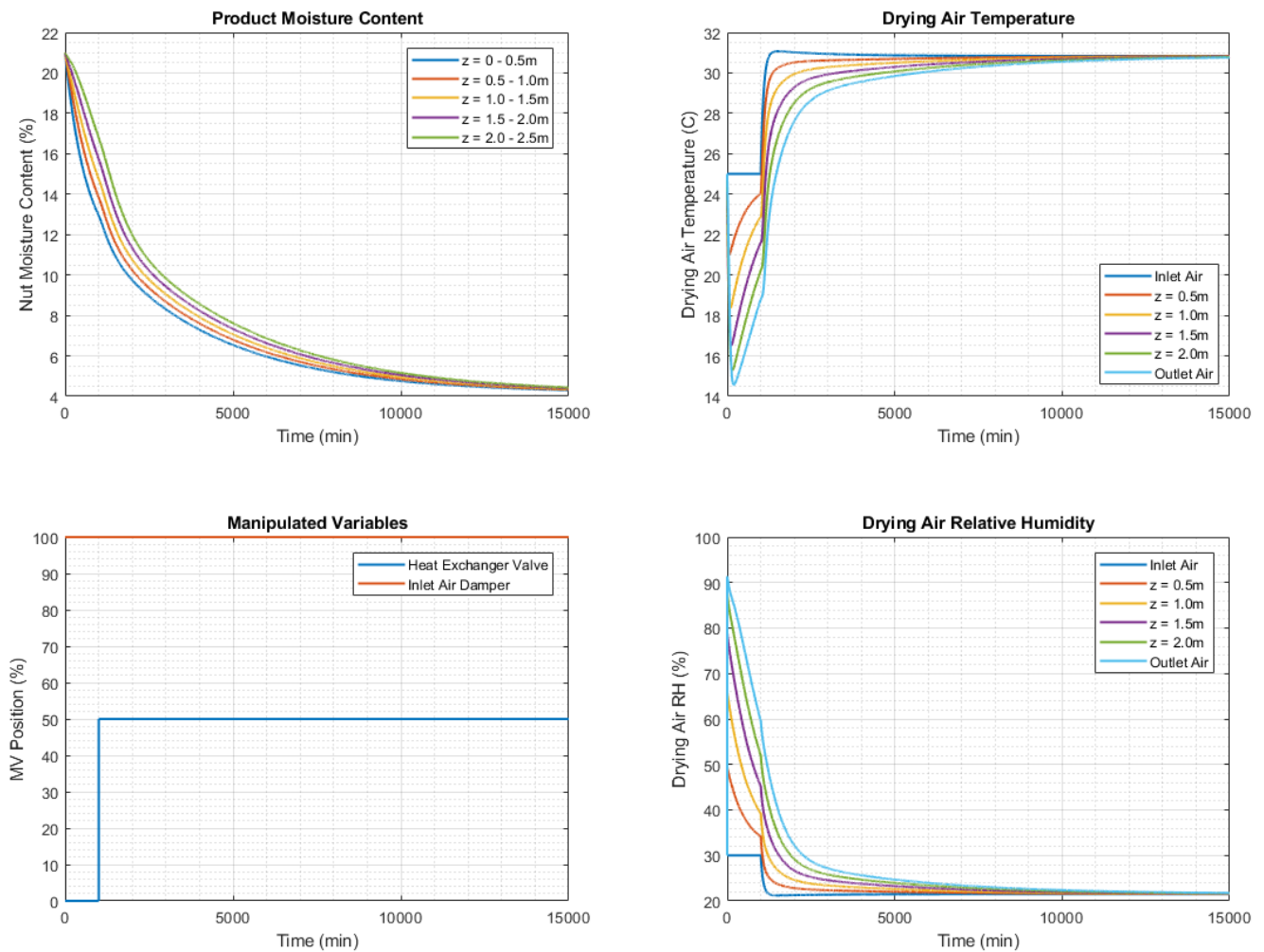


Figure 22: Open-loop simulation #3 - process reactions

Once again, the simulation qualitatively behaves as expected. The addition of heat to the inlet air causes a noticeable increase to the drying air's temperature. This of course lowers the relative humidity of that air, since it is able to hold larger quantities of moisture at higher temperatures. The end result is an increase to the rate of drying experienced by the product, as well as a lower equilibrium nut moisture content of around 4-5% (w.b.). Whilst the reactions appear to behave as expected, this must indeed be validated against actual plant data. The following chapter details a robust model verification exercise, which was undertaken to ensure the simulation is suitable for the purposes of control system design.

Chapter 7: MODEL VERIFICATION

It is not enough to simply develop a model or simulation and assume it works appropriately. This instead must be verified against plant data, ensuring the model exhibits some resemblance of the real system it is seeking to approximate. In the case of this project, plant data for five individual drying systems was available. This allowed for a robust verification exercise, ensuring that the model developed was transferrable between these systems.

7.1 DATA CLEANSING

The data that was received by the client for use in this project required a degree of “cleaning” before it could be fed through the MATLAB simulation for model validation. The data for each of the 5 silos provided contained roughly one and a half months of logged event data. Each silo had 15 Comma Separated Value (.csv) files containing a limited dataset of logged entries, retrievable from a Virtual Private Network (VPN) server. The entries themselves were not logged at regular time intervals, with data only being available for the process when a “significant event” had occurred. Furthermore, multiple, duplicate entries could exist for the same time interval, although the log comment field would be unique for each. A snapshot of how this data is formatted is given in Figure 23.

Thankfully, several key process values were conveniently formatted (silo temperature, relative humidity, heater valve position, etc.), which did not require any additional labour in extracting. However, this was not the case for all required values, since the comment field at the end of each entry contained crucial process information – encompassed within various text prompts. This included information such as the: ambient air condition, inlet damper position and VSD frequency to name a few. The log comment field often contained commas within the text itself, indistinguishable from the commas used in the .csv file structure. The data contained within this field is also very irregular, with process information only being available for a given time if it is included in that particular log entry.

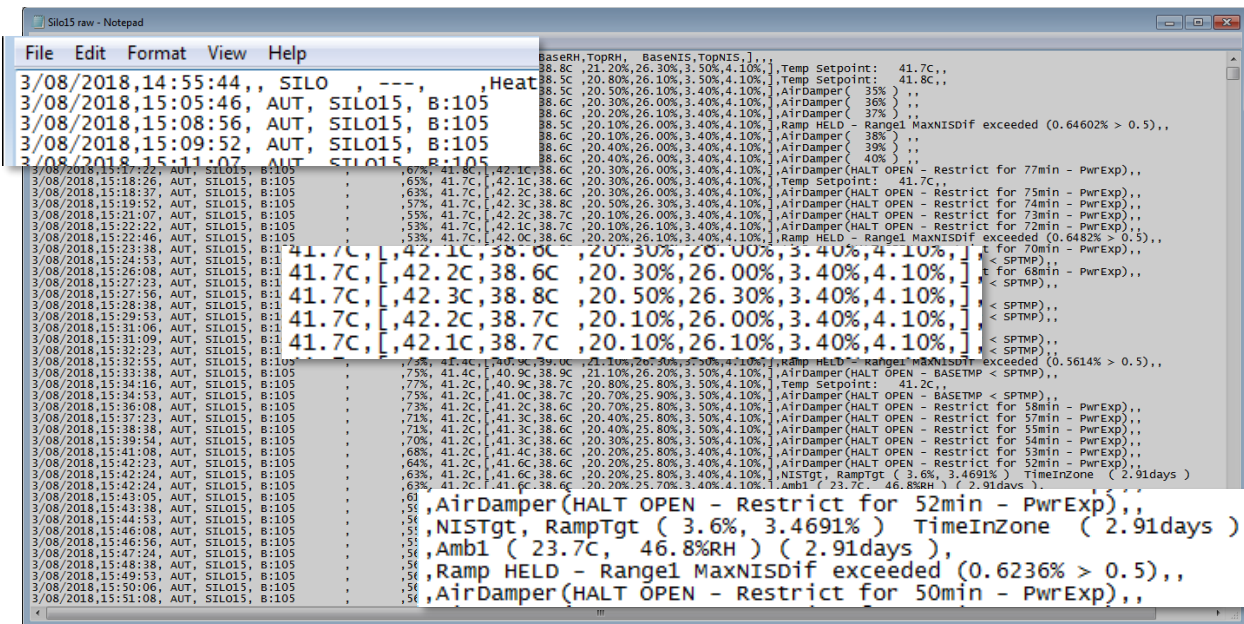


Figure 23: Snapshot of raw plant data formatting

Given the nature of this log data, the following tasks were conducted to format and homogenise the entries, ready for use in preceding simulations.

- The 15 partial log files for each silo were concatenated to create five continuous .csv log files (one for each silo).
- The data was imported into MS Excel, redundant fields were removed, and headings were associated to each field.
- The “Log Comment” data field was fixed by dynamically searching for commas in the right hand text entries. Commas within the .csv file which were not intended to indicate a new data field were distinguished from those that exist as part of the text in the log comment.
- The data for each silo was split into batches, provided that both a start and finish to that run could be identified within the data.
- A “Time Since Start” field was built in seconds for each run by unpacking and interpreting the date and time text entries within each log.
- The ambient air temperature, relative humidity, damper position and inlet fan VSD setting were distinguished within identifiable log comments, and extracted wherever possible into new data fields.

- Log entries that didn't explicitly follow the required format were individually removed from the batch data. This was usually due to the "Log Comment" data field incorrectly being placed where another parameter would normally be expected. Such an entry included indications of operating statuses, Auto/Manual mode select notifications and the like – not necessary for this project.
- All values to be extracted by MATLAB were copied into a fresh worksheet in Excel, with no formulas or data formatting. This was simply a precaution to ensure MATLAB extracted the values themselves, and not any formatting within a given cell.

An additional form of data cleansing was done in MATLAB. Upon opening the Excel file using the `xlsread()` function, data was selected for use in the simulation based on a few simple criteria. Firstly, the ability to enter a start-time was included, such that any data occurring prior to this time was omitted. Then any duplicate entries were removed from the validation dataset by testing whether subsequent logs were attained at the same time of the day. An exception to this was incorporated, so that if required information for a single time interval exists over multiple log entries, it may be included.

For some exercises, the data had to be interpolated since time intervals between each entry were so irregular. For the majority of parameters, values were interpolated using MATLAB's `interp1()` function. However, some parameters were changing as a direct result of the log itself and in such a case, a zero-order hold (ZOH) was more appropriate. For example, the ambient air temperature was attained periodically, so its value between logs is unknown – requiring an estimation using `interp1()`. On the other hand, all changes to the damper position were explicitly logged, so its value between time intervals is indeed known as it simply retains its previous value until another change is made – requiring the implementation of a zero-order hold. Figure 25 aims to better illustrate the difference between the two interpolation methods.

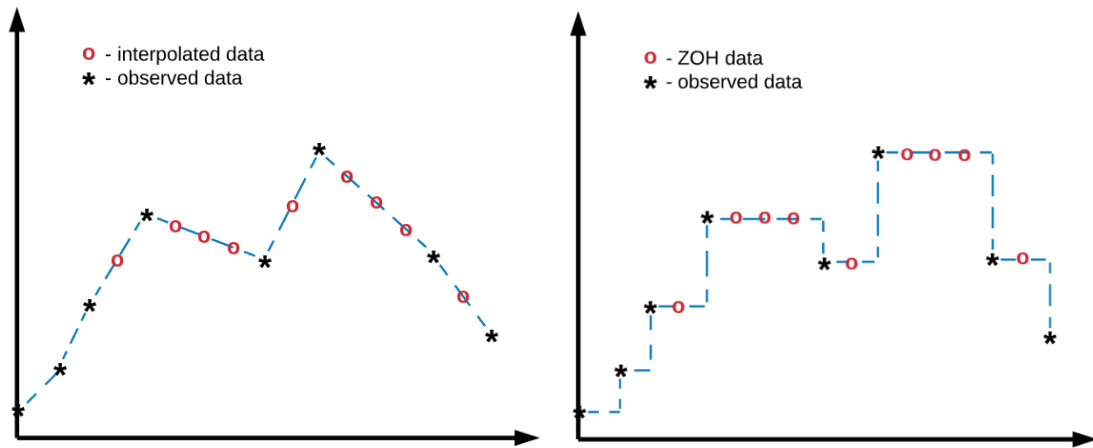


Figure 25: Difference between interpolation and a zero-order-hold

Before using MATLAB's system identification toolbox (as mentioned previously in Section 6.2.2), it was necessary to filter out high frequency components of the evaluation data. This was to improve MATLAB's ability to iterate toward an approximate heat exchanger process model, without suffering from excessively noisy data. Thankfully, MATLAB facilitates this exercise quite well, with the use of the `designfilt()` and `filtfilt()` functions. After interpolating a given set of data, these functions were deployed to provide the result exhibited by Figure 24.

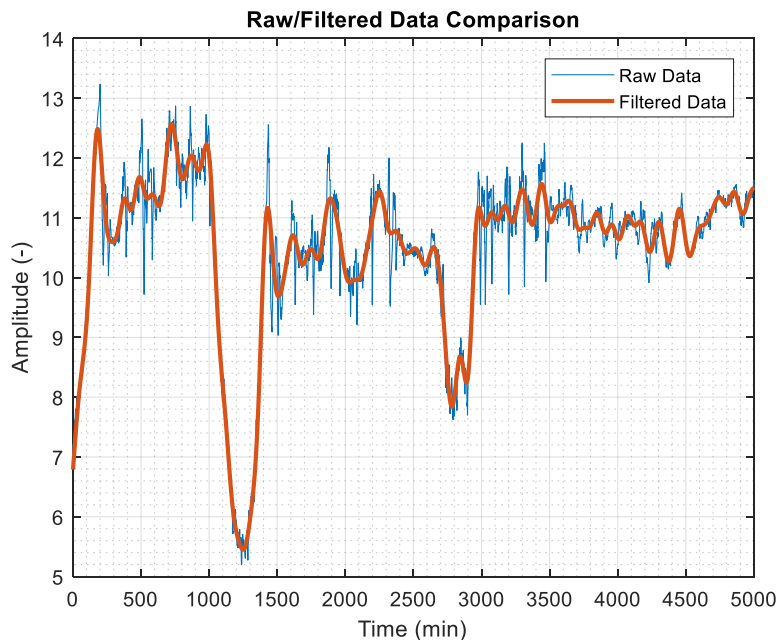


Figure 24: Filtering of noisy data for the use in MATLAB's system identification toolbox

This collates all the techniques used to attain an accurate, filtered and organised dataset, consisting of all available process values to be used in model validation. The dataset could be quickly modified to any batch across all silos for validation of every aspect of the process model.

7.2 VALIDATION OF MODEL OUTPUTS

This section aims to verify the model outputs for each subsystem, ensuring that the simulation is appropriate for use in control system design. The verification exercise was completed with a varied degree of success. It appears that whilst the simulation does indeed prove suitable for control system design, there are still deficiencies which could be addressed in future works. The nut drying process was validated in isolation to the subsidiary models created for the inlet air conditions, allowing a higher degree of granularity in assessing where model deficiencies exist.

7.2.1 NIS Macadamia Drying Process

Overall, the nut drying process model appears to be functioning at a high standard, with crucial process parameters closely following the qualities exhibited by the real system. However, it would appear that not all process dynamics have been captured entirely. This fact is most evident when analysing the top-bed air temperature assumed by the model, in comparison to that of the plant data. It appears that a temperature gradient exists over the nut-bed in reality, and yet this is not shown by the simulation.

For this subsystem, there are two available output parameters which can be used to verify the model, namely the top-bed's relative humidity and air temperature measurements. Plant data for the inlet air conditions was iteratively fed into the simulation, before the model calculated the resulting outlet air conditions. A comparison was then made to what was observed on the actual system. Figure 26 and Figure 27 exhibit both the simulation output and the associated plant measurement data for six batches across the five drying silos considered; plant data is shown in blue, and model data is shown in red.

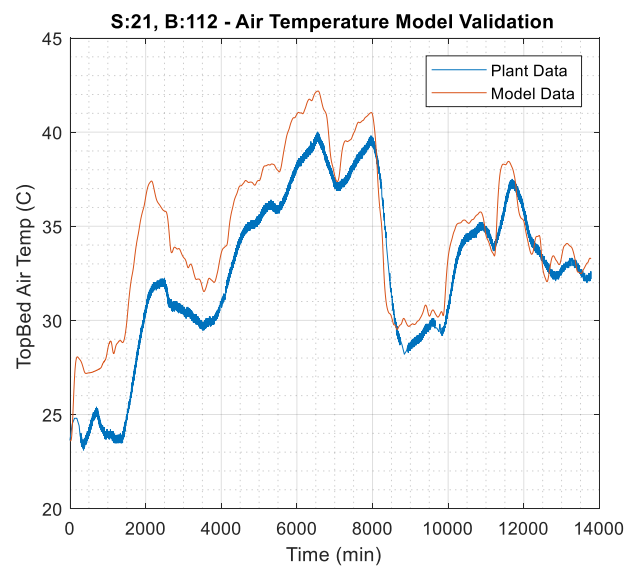
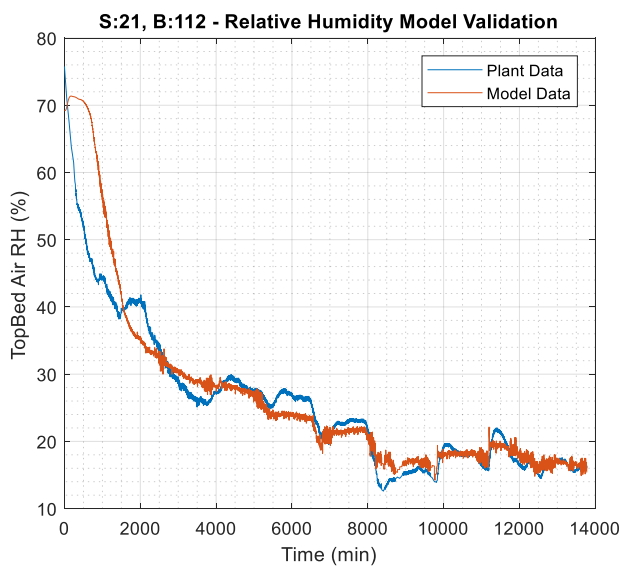
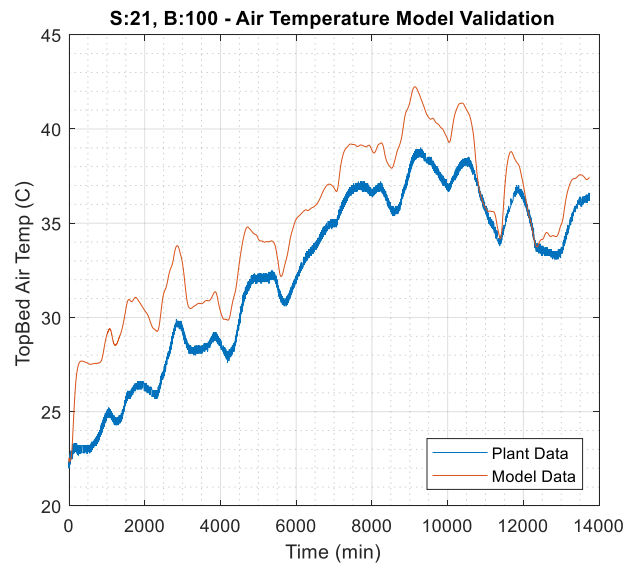
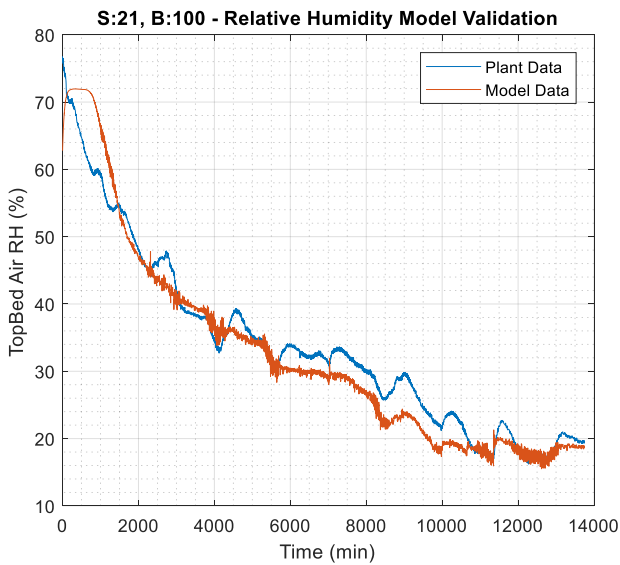
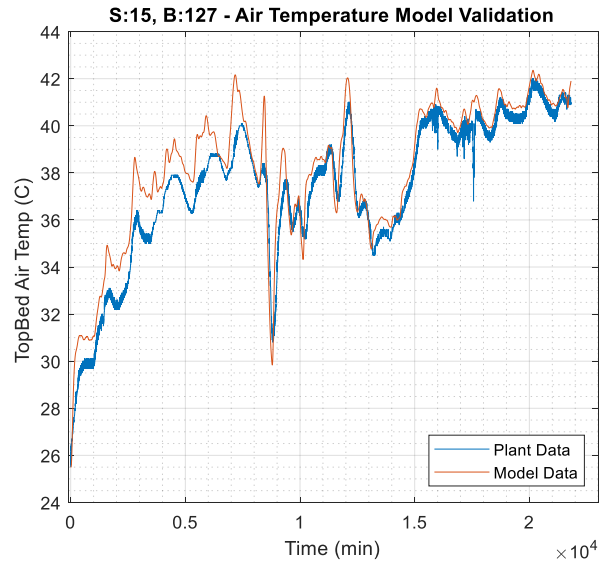
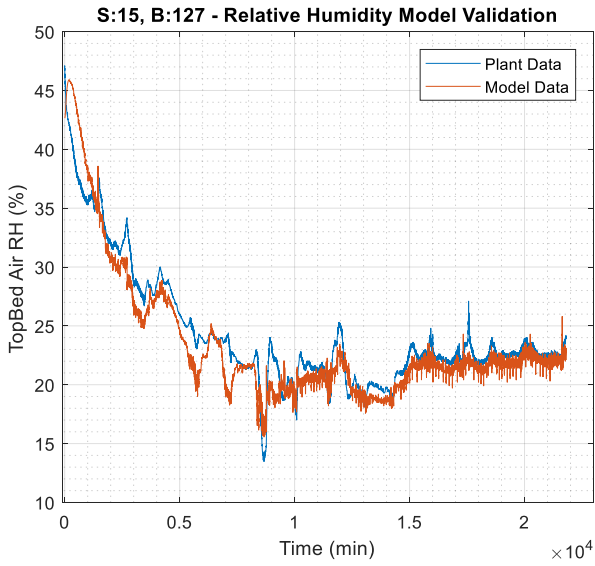


Figure 26: RH (left) and Temperature (right) validation curves; Silos 15 and 21, Batches 100, 112 and 127

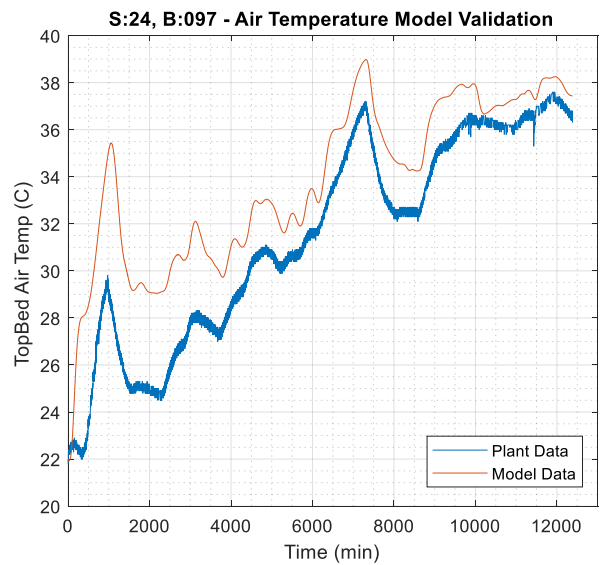
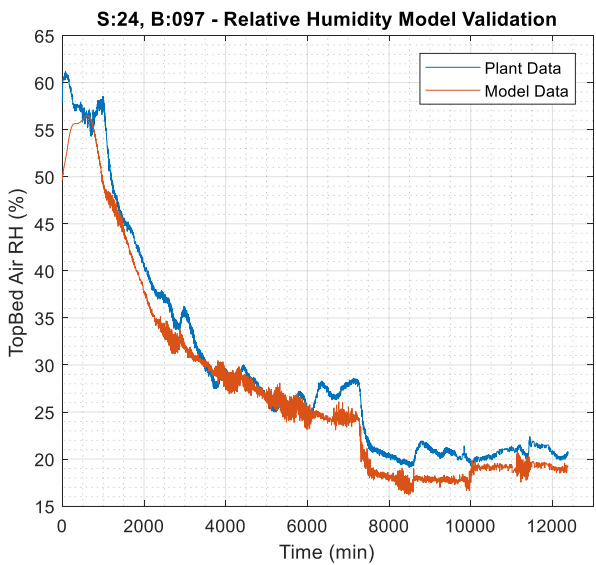
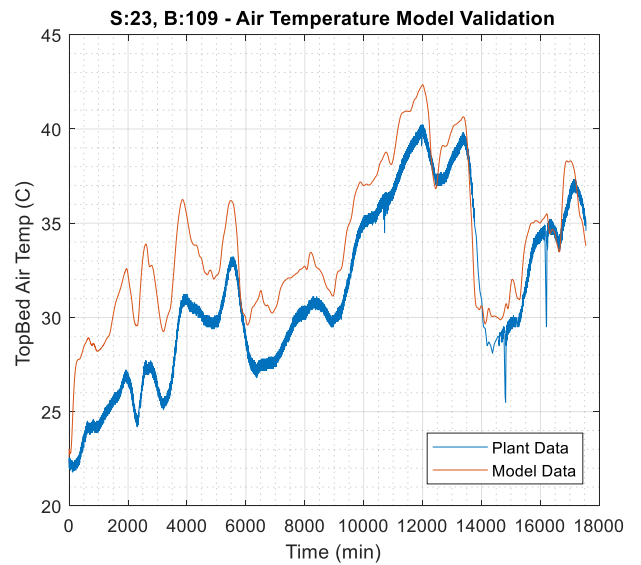
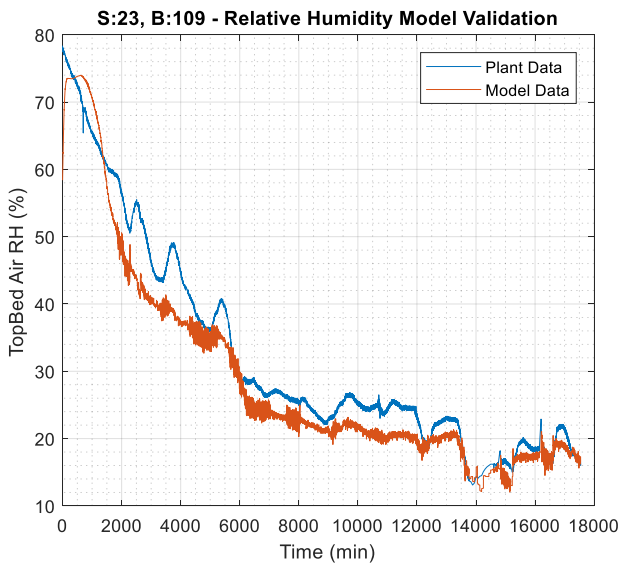
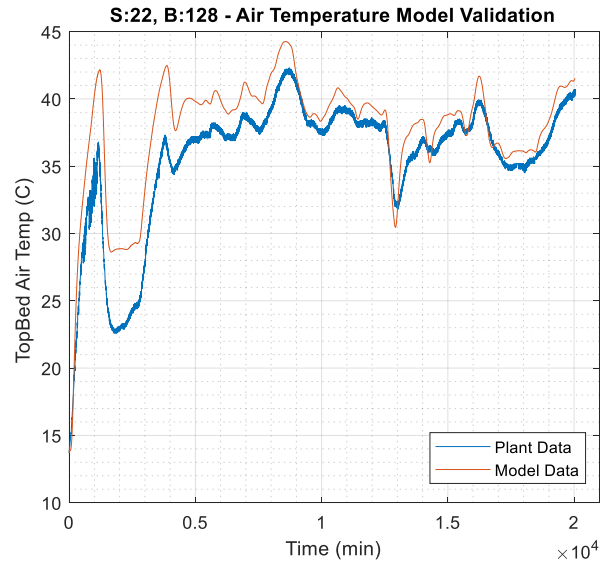
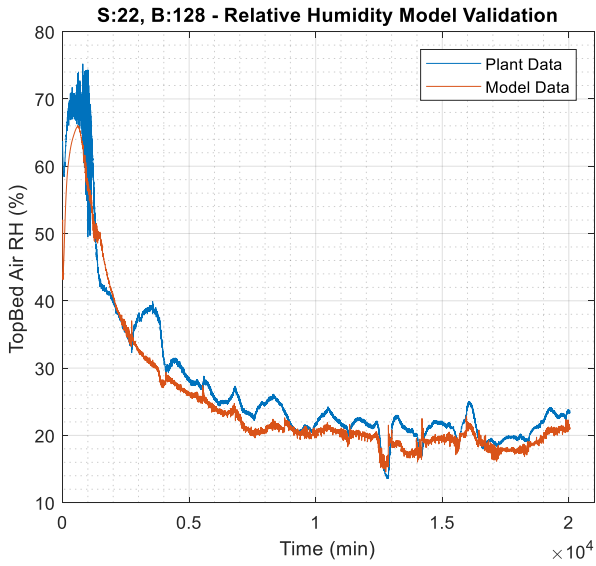


Figure 27: RH (left) and Temperature (right) validation curves; Silos 22, 23 and 24, Batches 097, 109 and 128

For all drying runs considered, the model appears to track the RH data very well, with a few caveats. At the start of every simulation there appears to be additional transients in the form of a “bump” which is not seen in the plant data. This is likely due to discrepancies in the initial steady state values throughout the model, along with the fact that the actual system has already commenced drying prior to $t = 0s$; thereby not exhibiting the same initial transients. The RH model responses do indeed have a similar dynamic response over both long-term and mid-term time intervals. But for the short-term response, it appears that the model may exhibit a higher magnitude of noise than what is seen in the plant data. With all of this taken into consideration, the model is still performing exceptionally well for the purpose of control system design. Quantifiable performance criteria for the RH model accuracy has also been evaluated and given in Table 5.

Table 5: Quantified performance data for RH model accuracy

Silo # / Batch #	Mean of Absolute Errors (MAE)	Implication
S:15 / B:127	1.4617 % _{RH}	The relative humidity data output from the model tracks that of the plant data very well.
S:21 / B:100	3.1301 % _{RH}	
S:21 / B:112	2.6286 % _{RH}	
S:22 / B:128	2.8893 % _{RH}	On average, the model is remaining within $\pm 2.65\%$; a result which is more than acceptable for the purpose of control system design.
S:23 / B:109	3.5274 % _{RH}	
S:24 / B:097	2.2521 % _{RH}	
Average:	2.6482 % _{RH}	

As eluded to earlier, the top-bed air temperature performs with a varied degree of success. The underlying dynamics of the model are arguably tracking the plant data very well, with matching peaks and troughs appearing consistently across the board. However, there exists a noticeable offset in temperature between the simulation and plant data, especially for earlier time periods. Upon further investigation, it was found that the simulation is not adequately capturing the gradient in temperature that exists across the height of the nut-bed. To illustrate this, Figure 28 shows the difference in temperature from top to bottom of the nut-bed for both the plant (left) and model (right) data.

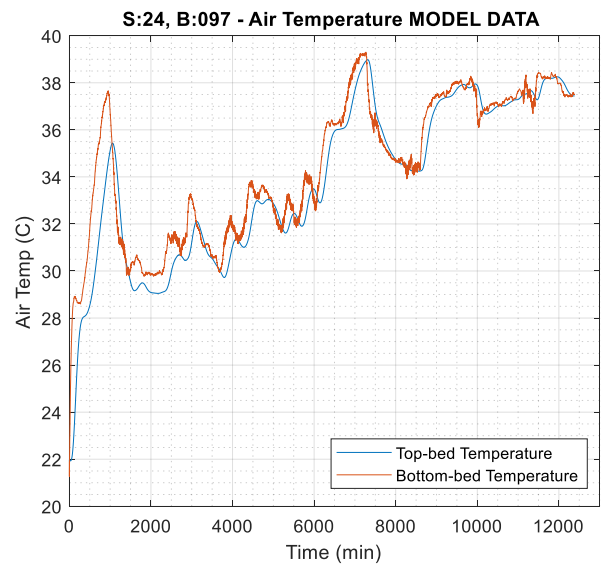
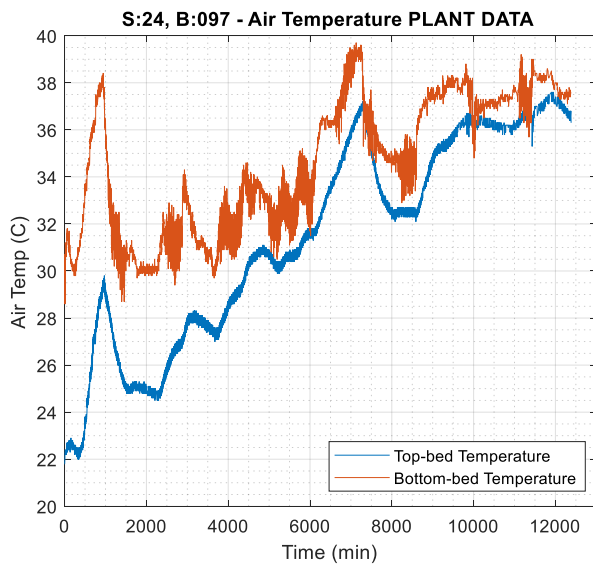


Figure 28: Comparison of the temperature gradient exhibited by plant data vs model data

It is clearly evident that something is amiss within the simulation. It can be seen that for early stages in drying, the plant data exhibits a temperature gradient across the nut-bed which is not present in the model. As the product continues to approach its equilibrium moisture content, this gradient begins to decrease in magnitude. It is suspected that perhaps a crucial aspect of the process dynamics has been omitted from the model equations, resulting in this deviation. Perhaps there exist additional qualities of macadamia nuts – not present within hazelnuts – which demand the modification of the model structure in order to accurately represent this behaviour. The simulation has been rigorously checked against the information given within literature, and extensively analysed for faults which may cause this error. But to the best of the author’s knowledge, the simulation is operating “as intended”. Given more time and resources, this issue could be further investigated and potentially rectified. As was done for relative humidity, Table 6 gives a quantified performance evaluation of the model’s temperature data.

Table 6: Quantified performance data for temperature model accuracy

Silo # / Batch #	Mean of Absolute Errors (MAE)	Implication
S:15 / B:127	1.0362 °C	The temperature data output from the model tracks that of the plant data moderately.
S:21 / B:100	2.6097 °C	
S:21 / B:112	2.2797 °C	On average, the model is remaining within $\pm 2.25^\circ\text{C}$. Whilst this is a comparatively larger discrepancy than that of RH, it should not have a detrimental effect on control system design.
S:22 / B:128	2.2748 °C	
S:23 / B:109	2.4777 °C	
S:24 / B:097	2.8297 °C	
Average:	2.2512 °C	

Despite the discrepancies observed on the outlet air temperature, the model is expected to adequately serve its purpose in control system design. The temperature shown by the model still exhibits the same mid-term dynamics as the actual process, which is the main area of concern for this control system. In reality, this quantity will be measured and not calculated, so its value will be known. Perhaps the most significant implication of this result would be in the implementation of a model based controller. Under such a control scheme, this deviation from plant dynamics may induce poor control performance, since such controllers rely on a high degree of plant-model accuracy.

7.2.2 Inlet Air Conditions

The verification of the subsidiary models concerning the inlet air is simple in comparison to that of the nut drying process. Firstly, neither the inlet mixing point nor the inlet heat exchanger can be verified in isolation. This is because no measured plant data exists for the midway point which exists after the mixing point and before the heat exchanger. The model for the mixing point has been built under assumptions which make it easier to define the system, but of course this implies it may not perfectly represent its actual dynamics. However, the approach was conducted with a firm theoretical basis and thus any deviation from the actual plant dynamics is considered to be negligible.

Despite not being able to confirm the output of the mixing point directly, it is inherently verified if both the mixing point and the heat exchanger are considered simultaneously. Firstly, the prior

assumption that the recycle stream's air condition is equal to that of the top-bed air condition is maintained. This accompanied by the fact that both the ambient air and bottom-bed air conditions are explicitly measured, provides a means to validate this model. In fact without these variables, these processes could not have been modelled using the system identification method outlined in Appendix B. A filtered dataset for deviations in bottom-bed air temperature (as per the methods discussed in Section 7.1) was used in both the modelling and verification exercises. This deviation is of course how the air temperature leaving the mixing point has been affected after interacting with the heat exchanger. A comparison between this dataset and the corresponding output for the two subsidiary process models (connected in series) is given in Figure 29.

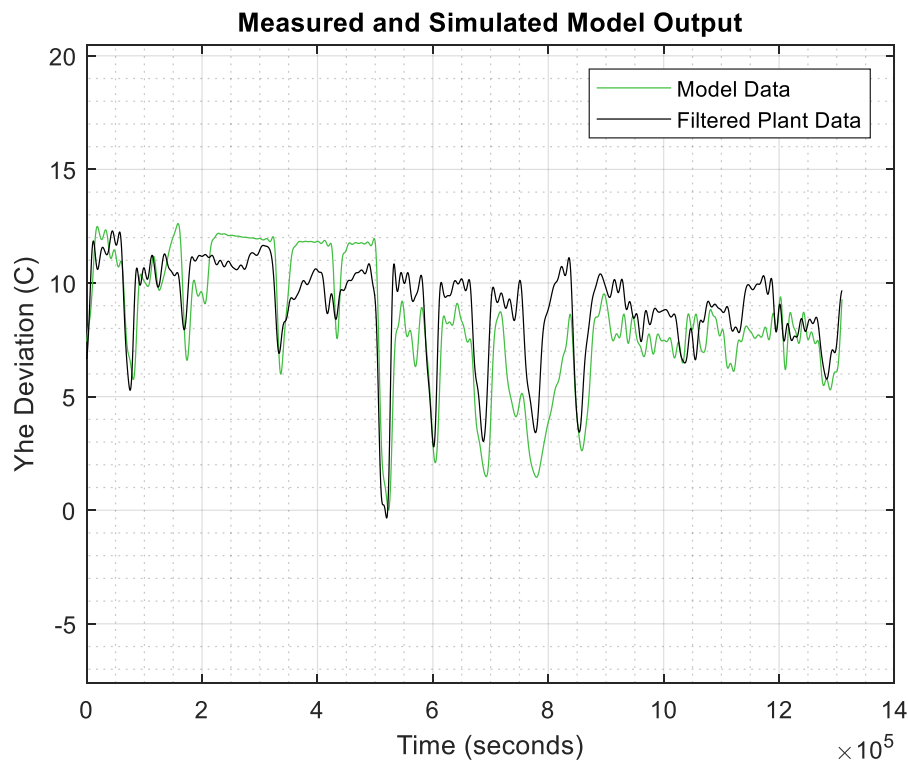


Figure 29: Inlet air model validation data comparison

Qualitatively, the model output appears to track the plant data reasonably well. Of course since this is only an approximation it should not be expected to track the physical system precisely, but it is reassuring nonetheless to see the system respond in a similar way to what is expected. Evidently, some model deficiencies do indeed exist. Yet for the purpose for control system design, the approximation appears to produce a suitable output. The various peaks and troughs are roughly

represented, with an appropriate speed of response in both a short and long term timescale. As given for the previous model validations in Table 5 and Table 6, the mean of absolute errors for this model is ± 1.67 °C, implying a reasonable fit to the verification data.

Chapter 8: CONCLUSION

This final chapter aims to summarise work conducted throughout the project. It has been the intention of the author to provide a detailed analysis of various project components as they have been introduced. However, two important topics yet to be discussed is that of barriers to completion, and future improvements. The deliberation of these concluding topics will lead into the summarising statements which close the body of this document.

8.1 ISSUES, CHALLENGES AND BARRIERS

A significant barrier to completion was in the acquisition and adaptation of plant data, necessary for model validation. The data was delivered at roughly the midway point of the project, which in truth did leave plenty of time to conduct model validation. However, the extent to which the data would have to be cleaned and modified was not anticipated. This set back the ability to accurately verify model components, given the large amount of programming overhead which was required to complete this task. As an aside to this, had the data been delivered at the very beginning of the project, then perhaps an empirical process model could have been developed for the entire process from the outset. If done successfully, this would leave time to design a control system without the need to conduct the cumbersome process of modelling by fundamental principles. However, it was the original intention of the client for such a modelling exercise to take place, so the delivery time of the data was indeed appropriate. The shift to an empirical model at the midway point was not considered to be an option since it required the abandonment of roughly two and a half months of good quality work.

On a more general note, the modelling and simulation procedures were of a much higher complexity than what was initially foreseen. It could be at the fault of the author for “diving to deep” but this is not believed to be the case. All the model components, programming techniques, research and analysis throughout this project have been necessary for its success. In fact, as it will be shown in the upcoming section pertaining to future works, there are indeed components of this project which could yet be modified to add further value. It was testing to question the validity of modelling resources

found in journal articles, since this was assumed to be an authoritative source of information. However, after scrutinising the works of various authors, it is now clear that not all publications are created equal and minor mistakes do indeed appear in published literature. As a final comment, it was found that despite being the most daunting aspect initially, the derivation of model equations was only ever half the story. The ability to transfer such concepts programmatically into a simulation was often of equal complexity and importance.

8.2 FUTURE WORKS

As with most engineering endeavours, there is still plenty which can be done to both improve and expand the work conducted in this thesis. The future works as identified by the author have been broken into two parts; one for the improvement of work conducted within this project, and another for the design of an accompanying control system. These sections will hopefully be of great value for anyone wanting to carry forward the work in this project.

8.2.1 Improving the Model and Simulation

Despite the best efforts of the author to create a robust model and simulation, there is still some areas which could be improved by future collaborators. Some suggestions on where best to focus such improvements are detailed below:

- It has been mentioned that the use of the `fzero()` function to estimate t_{eq} has caused some intermittent crashing issues. The root cause of this was not able to be determined, so this could be further investigated to diagnose the issue, and design a better method of calculating t_{eq} . One potential modification is to approximate the “two-term exponential” thin-layer drying rate equation (3.1) as a Page equation variant – like that of equation (5.1). This could then allow the rearrangement of the Page equation to explicitly solve for t_{eq} as shown in equation (5.6), which was not possible with the two-term exponential form. The correction

of this issue would allow model verification to be conducted without the need for the workaround given in Appendix C, and reduce the risk of simulation crashes.

- It was found in research and mentioned in Section 3.2 that air velocity plays a negligible role in affecting the rate of drying. This was not investigated in detail, so another suggestion is to include this aspect in the model, and then verify it within the simulation. Ideally it would be beneficial to attain plant data pertaining to pressure and air velocity to assist in this, but this may not be feasible. The simulation already performs quite well, but this inclusion will aid in either confirming or discrediting the theory that the effect of air velocity is negligible.
- The heat exchanger's approximate model may not be suited to process conditions that deviate far from those to which it was empirically derived. This is perhaps the weakest point in the simulation and could certainly be improved by a more theoretical modelling approach. An investigation could be made as to whether enough process information is known to formulate a theoretical model. Ideally this would include operating plant data on the heating medium, and physical properties of the heat exchanger. Such a modification is likely to greatly improve the simulation's ability to accurately estimate process conditions.
- Two aspects of Lopez's simulation for hazelnuts [21], which were not included in this simulation are that of shrinkage and rewetting. In the case of the latter, this should already be handled by the thin-layer drying model; if the calculated equilibrium moisture content is greater than the present nut moisture content, then this results in commensurate rewetting. Shrinkage on the other hand, was considered to be negligible in this model so no such scheme was deduced for macadamias. The inclusion of shrinkage and/or rewetting is not expected to be of great impact to the model, but could be an improvement nonetheless.

8.2.2 Control System Design

The most significant piece of future work that should be attempted by future collaborators is that of control system design. There would be enough content here to potentially write an entirely separate

thesis, but it may be the desire of the client to conduct this themselves. Given herein is an overview of how this task can be approached and the different aspects which should be considered.

The first task to be completed is that of interaction analysis, so the pairing of MVs and PVs can be determined. Interestingly, since both the damper and heat exchanger affect both temperature and relative humidity, one might find that the most suitable pairing under one set of operating conditions is the opposite to another. Either a pairing which satisfies the majority of operating conditions could be chosen, or perhaps a system which has the ability to dynamically switch MV-PV pairs could be developed. Of course such a system should include bumpless transfers and other relevant safe guards to ensure the system does not behave erratically.

After pairing, the structure of individual control loops should be defined. The most simple to implement would be conventional feedback loops with PID controllers. This may be the most suitable type of controller given that the process should not be expected to be too complex on a loop-by-loop basis. However, if the model can be leveraged to create a Generic Model Control (GMC) scenario, this may have the ability to vastly outperform the abilities of a PID controller. The fact that such a comprehensive model has been derived makes this option tempting, but deriving the GMC scheme may be a difficult task – worthy of looking into nonetheless. Dynamic Matrix Control and other forms of advanced, model predictive control methods could be investigated, especially if optimisation and online model improvements are desirable.

After the control system architecture has been chosen, the simulation should be modified to include the closed-loop structures, and controllers should be tuned. Such modifications will be dependent on which type of controllers are going to be tested. For the most part, this is not too difficult. In fact, some quick modifications were made to the current simulation to include conventional feedback loops and PID controllers to test the ease of such a task. Figure 30 provides the response of a simple feedback control scenario after a setpoint change of 5°C to inlet air temperature, via the heat

exchanger's control valve to prove this. The code for all programs have been submitted electronically if the reader would like to look over how such modifications are made.

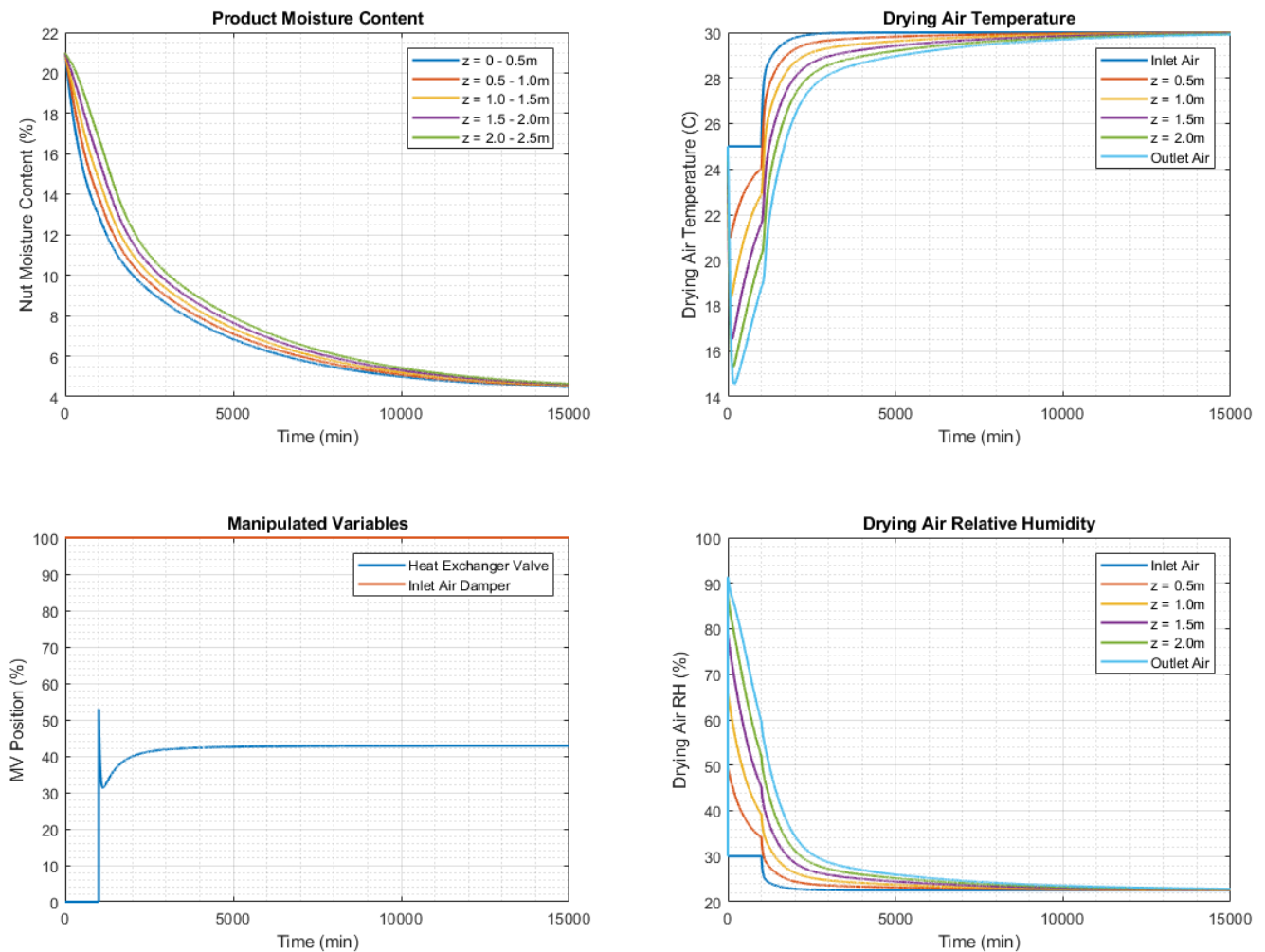


Figure 30: Example response for a closed-loop conventional feedback control scenario ($K_c = 0.10521$, $\tau_{u_i} = 267.5056$, $\tau_{u_D} = 0$)

The next task should be to develop how the algorithm makes decisions on the most suitable control actions as the product dries. This would likely take the form of a predefined rule base, with the different conditions that determine what drying regimes are used and when. At this time, optimisation and economics should also be considered. An ambitious addition would be to include an artificial intelligence (AI) that learns how to adjust and improve this rule base over time. Such an AI would likely take the form of an artificial neural network.

The resulting control system would have to be rigorously tested using the drying simulation. This could even be simulated under “real” conditions, feeding the already acquired ambient air data into the

simulation to act as a disturbance. This would test whether the algorithm is making appropriate decisions toward how to change its drying strategy as conditions change throughout the drying period. After the control system has been developed, it would then have to be adapted into hardware, whether it be a programmable logic controller (PLC) or some separate standalone physical application.

8.3 CONCLUDING REMARKS

The drying of agricultural produce can be a deep and substantive field of study. Pressure remains on the Australian macadamia industry to continually innovate drying technologies, in order to remain a global market leader in macadamia exports. Macadamias are quite susceptible to degradation, which has been shown to be a direct result of drying and storage techniques. The development of an accurate process model allows engineers to better understand the drying kinetics of the crop, and thereby produce a more efficient control system. Throughout this report, evidence has been given toward the research and design of a model and simulation for the drying of nut-in-shell macadamias. The model developed in this study was shown to operate at a high level of accuracy, with the accompanying simulation performing very well for the purposes of control system design. Thus, the project aims stated in Chapter 1 have indeed been met successfully.

The report opened with a background discussion about the Australian macadamia industry and the importance that drying plays in the post-harvest chain of operations. The topic of modelling was extensively reviewed, discussing the most suitable techniques currently employed by researchers to model such systems. Importance was placed on both thin-layer and deep-bed modelling, and how these two techniques have been commonly leveraged to develop drying simulations for other food crops. The topic of control system design was briefly discussed. Whilst no final control system was developed during this project, the simulation has indeed been developed with the intention to facilitate future control design efforts.

After gathering various modelling components and information from literature, it was deemed necessary to first recreate this work. Constructing the model in a piece-by-piece manner was important to ensure that any issues were identified and corrected early. Only once each component had been developed, tested and understood were they considered for inclusion in the final drying model for macadamias. The overall open-loop structure was studied and subsidiary processes were identified. Then a sideward modelling discussion was given for these smaller processes, so that their dynamics may be approximated and included in the final simulation. Most of the modelling components found in literature were concerned with drying the nut specifically, with little consideration given toward manipulated variables. Some extra considerations toward how the model had to be adapted into a simulation were given. The majority of work in this thesis was in the implementation of theoretical concepts into a programming environment, so the different nuances in doing so were discussed at length. No modelling or simulation design exercise is complete without a robust verification procedure. The techniques, results and subsequent implications were deliberated, eventually determining that the simulation is indeed suitable for control system design. Data cleansing became another significant topic, since this process became so integral to the entire modelling and verification procedure. Finally, this chapter has aimed to provide a reflection on the project itself. Barriers to completion were discussed, and a comprehensive section was given toward future works for this project.

The author maintains the opinion that the work within this thesis is of a high standard. The primary modelling exercises have a firm theoretical basis and are well grounded by supporting literature. Any assumptions and approximations have been adequately noted and concessions have been given toward their performance if appropriate. The intention of this report was not to provide an exhaustive programming tutorial, but instead discuss the reasoning and application behind such techniques. As such, the methods of design and implementation given throughout this work have been collated with a high attention to relevancy. Additionally, the verification procedure used to prove the quality of this work has been robust and thorough. A comprehensive discussion was given toward the project's

shortfalls and future work was discussed at length, such that future students and collaborators may benefit from this information. Hopefully the model and simulation developed here will be of use to the project client, and a high performing control application may be developed in the future using this utility.

BIBLIOGRAPHY

- [1] Australian Macadamia Society Ltd, "About The Macadamia Industry," Australian Macadamia Society Ltd, 2017. [Online]. Available: <https://www.australianmacadamias.org/industry/about/about-the-macadamia-industry>. [Accessed 10 Sep 2018].
- [2] Horticulture Innovation Australia Ltd, Australian Horticulture Statistics Handbook: Nuts, Sydney, NSW: Horticulture Innovation Australia Ltd, 2016.
- [3] Australian Macadamia Society Ltd, "Australian Production," Australian Macadamia Society Ltd, 2018. [Online]. Available: <https://www.australianmacadamias.org/industry/facts-figures/australian-production>. [Accessed 20 Aug 2018].
- [4] J. A. Moses, T. Norton, K. Alagusundaram and B. K. Tiwari, "Novel Drying Techniques for the Food Industry," *Food Engineering Reviews*, vol. 6, no. 3, pp. 43-55, 2014.
- [5] H. M. Wallace and D. A. Walton, "Macadamia (Macadamia Integrifolia, Macadamia Tetraphylla and Hybrids)," in *Postharvest Biology and Technology of Tropical and Subtropical Fruits*, Sawston, Cambridge, UK, Woodhead Publishing Limited, 2011, pp. 450-473.
- [6] J. Wilkinson, "Macadamias," in *Nut Grower's Guide: the complete handbook for producers and hobbyists*, Collingwood, VIC, Australia, Landlinks Press, 2005, pp. 150-167.
- [7] Australian Macadamia Society Ltd, "Fact Sheet 2: Drying Macadamia NIS On-Farm," Australian Macadamia Society, Lismore, NSW, Australia, 2009.
- [8] Machine & Process Design, "Bulk Density," MPD-Inc.com, 2015. [Online]. Available: <http://www.mpd-inc.com/bulk-density/>. [Accessed 17 Aug 2018].

- [9] Knowledge Revolution, "Isotherm BET/GAB," KnowledgeRevolution.com.au, 10 Aug 2008.
[Online]. Available: <http://www.knowledgerevolution.com.au/Isotherm%20BETGAB.htm>.
[Accessed 17 Aug 2018].
- [10] Vaisala, "Humidity Conversion Formulas," Vaisala, Helsinki, Finland, 2013.
- [11] K. Palipane and R. Driscoll, "Moisture Sorption Characteristics of In-Shell Macadamia Nuts,"
Journal of Food Engineering, vol. 18, no. 1, pp. 63-76, 1992.
- [12] P. O'Hare, K. Quinlan, R. Stephenson, N. Vock, H. Drew, J. Ekman, D. Firth, E. Gallagher, P.
O'Farrell, P. Rigden, C. Searle, I. Vimpany and G. Waite, "Chapter 3: Growing the Crop," in
Macadamia Information Kit. Agrilink, your growing guide to better farming guide, Brisbane,
QLD, Australia, Queensland Horticulture Institute, 2004, pp. 17-70.
- [13] Australian Macadamia Society Ltd, "Fact Sheet 3: Silo Modifications to Improve Efficiency and
Kernel Quality," Australian Macadamia Society, Lismore, NSW, Australia, 2010.
- [14] M. Le Lagadec, "Kernel Brown Centres in Macadamia: A Review," *Crop and Pasture Science*,
vol. 60, no. 12, pp. 1117-1123, 2009.
- [15] D. Bungay, *Macadamias: Guide to On-Farm Post-Harvest Care*, Tzaneen: The South African
Macadamia Growers Association, 2003.
- [16] Z. H. Wang and G. Chen, "Heat and Mass Transfer in Fixed-Bed Drying," *Chemical Engineering
Science*, vol. 54, no. 1, pp. 4233-4243, 1999.
- [17] Z. Erbay and F. Icier, "A Review of Thin Layer Drying of Foods: Theory, Modeling, and
Experimental Results," *Critical Reviews in Food Science and Nutrition*, vol. 50, no. 5, pp. 441-
464, 2010.

- [18] K. Palipane and R. Driscoll, "The Thin-Layer Drying Characteristics of Macadamia In-Shell Nuts and Kernels," *Journal of Food Engineering*, vol. 23, no. 2, pp. 129-144, 1994.
- [19] Y. Sahari and R. Driscoll, "Thin Layer Drying of Agricultural Products: A Review," in *3rd Malaysian Postgraduate conference*, Sydney, NSW, Australia, 2013.
- [20] P. Pankaew, S. Janjai, W. Nilnont, C. Phusampao and B. Bala, "Moisture Desorption Isotherm, Diffusivity and Finite Element Simulation of Drying of Macadamia Nut (*Macadamia Integrifolia*)," *Food and Bioproducts Processing*, vol. 100, no. 1, pp. 16-24, 2016.
- [21] A. López, M. Piqué and A. Romero, "Simulation of Deep Bed Drying of Hazelnuts," *Drying Technology*, vol. 16, no. 3-5, pp. 651-665, 1998.
- [22] I. Istadi and J. P. Sitompul, "A Comprehensive Mathematical and Numerical Modeling of Deep-Bed Grain Drying," *Drying Technology*, vol. 20, no. 6, pp. 1123-1142, 2002.
- [23] A. López, P. Virseda, G. Martinez and M. Llorca, "Deep Layer Malt Drying Modelling," *Drying Technology*, vol. 15, no. 5, pp. 1499-1526, 1997.
- [24] M. Nellist, "The drying of ryegrass seeds in deep layers," Newcastle University, Newcastle, UK, 1974.
- [25] J. P. Sitompul, Istadi and I. N. Widiassa, "Modeling and Simulation of Deep-Bed Grain Dryers," *Drying Technology*, vol. 19, no. 2, pp. 269-280, 2001.
- [26] M. Omid, A. Baharlooie and H. Ahmadi, "Modeling Drying Kinetics of Pistachio Nuts with Multilayer Feed-Forward Neural Network," *Drying Technology*, vol. 27, no. 10, pp. 1069-1077, 2009.

- [27] G. S. Srzednicki, R. Hou and R. H. Driscoll, "Development of a control system for in-store drying of paddy in Northeast China," *Journal of Food Engineering*, vol. 77, no. 2, pp. 368-377, 2006.
- [28] C. Li, H. Ban and W. Shen, "Self-Adaptive Control System of Grain Drying Device," *Drying Technology*, vol. 26, no. 11, pp. 1351-1354, 2008.
- [29] O. F. Lutfy, H. Selamat and S. B. M. Noor, "Intelligent Modeling and Control of a Conveyor Belt Grain Dryer Using a Simplified Type 2 Neuro-Fuzzy Controller," *Drying Technology*, vol. 33, no. 10, pp. 1210-1222, 2015.
- [30] M. Aghbashlo, S. Hosseinpour and A. S. Mujumdar, "Application of Artificial Neural Networks (ANNs) in Drying Technology: A Comprehensive Review," *Drying Technology*, vol. 33, no. 12, pp. 1397-1462, 2015.
- [31] Engineering Toolbox, "Water - Thermophysical Properties," Engineering Toolbox, 2003. [Online]. Available: https://www.engineeringtoolbox.com/water-thermal-properties-d_162.html. [Accessed 23 October 2018].
- [32] I. Urieli, "Specific Heat Capacities of Air," 2008. [Online]. Available: https://www.ohio.edu/mechanical/thermo/property_tables/air/air_cp_cv.html. [Accessed 23 October 2018].
- [33] Engineering ToolBox, "Water Vapor - Specific Heat," Engineering ToolBox, 2005. [Online]. Available: https://www.engineeringtoolbox.com/water-vapor-d_979.html. [Accessed 23 October 2018].
- [34] C. E. Bullock and L. L. Geer, "Chapter 6: Psychrometrics," in *ASHRAE Fundamentals*, Atlanta, GA, American Society of Heating, Refrigerating and Air-Conditioning Engineers, Inc., 1985, pp. 6.4, 6.8-6.10.

- [35] Engineering ToolBox, "Mixing Humid Air," EngineeringToolBox.com, 2004. [Online]. Available: https://www.engineeringtoolbox.com/mixing-humid-air-d_694.html. [Accessed 3 November 2018].
- [36] A. Becker, "Solving a sum of exponentials," Stack Exchange, 2012. [Online]. Available: <https://math.stackexchange.com/questions/129504/solving-a-sum-of-exponentials>. [Accessed 29 October 2018].
- [37] C. Borompichaichartkul, K. Luengsoke, N. Chinprahast and S. Devahastin, "Improving Quality of Macadamia Nut (*Macadamia Integrifolia*) Through the Use of Hybrid Drying Process," *Journal of Food Engineering*, vol. 93, no. 3, pp. 348-353, 2009.
- [38] F. Kong and R. Singh, "12 - Advances in instrumental methods to determine food quality deterioration," in *Food and Beverage Stability and Shelf Life*, Sawston, Cambridge, UK, Woodhead Publishing Ltd., 2011, pp. 381-404.
- [39] Y. Wang, L. Zhang, J. Johnson, M. Gao, J. Tang, J. R. Powers and S. Wang, "Developing Hot Air-Assisted Radio Frequency Drying," *Food and Bioprocess Technology*, vol. 7, no. 1, pp. 278-288, 2014.
- [40] F. Silva, M. Silva, A. Marsaioli, G. Maximo and L. Gonçalves, "Microwave assisted drying of macadamia nuts," *Journal of Food Engineering*, vol. 77, no. 3, pp. 550-558, 2006.
- [41] M. Weidman, "Zero-Order Hold," MathWorks, 15 January 2014. [Online]. Available: <https://au.mathworks.com/matlabcentral/fileexchange/45040-zero-order-hold>. [Accessed 3 November 2018].

APPENDIX

A. NOVEL DRYING TECHNOLOGIES

Aside from the conventional system described in Section 2.2.1, there are other food drying technologies which have the potential to improve the drying of macadamia nuts. Moses et al. [4] have given a comprehensive review on some of these technologies, their operation and how they may be leveraged for use in the food industry. Methods of drying such as: ultrasound assisted, microwave assisted, refractance window, superheated steam, high electric field, infrared and heat pump drying are presented [4]; some of which, have been tested by other researchers on macadamias specifically.

Borompichaichartkul et al. [37] suggested the use of a hybrid drying process which utilised heat pump drying at 40°C, followed by hot-air drying at 50-70°C. The authors propose that this method may improve drying times without adversely affecting quality, but large deviations in the product's peroxide value suggest that the flavour of the nuts dried in this manner may have changed [38]. The industry's current reliance on peroxide value and fatty free acid (FFA) analysis in the diagnosis of rancidity is generally deemed to be inadequate, with a sensory evaluation still being the most reliable testing method [5]. No such evaluation was given in Borompichaichartkul's paper.

Wang et al. [39] proposed a hot-air assisted radio frequency (RF) drying scheme with mixed results. The pilot scale drying system utilised a system of 27 MHz RF electrodes in conjunction with a through-flow hot-air drying setup. Again, this method showed a reduction in drying time but with increases to both the peroxide value and FFA content [39]. The authors note that the final measured values remain within industry limits, with the concession that these values appear to carry on rising as the drying process continues [39]. A similar study was conducted on a microwave hybrid system, with associated sensory evaluations proving to have positive results [40]. The method does show promise, but more research needs to be done on the feasibility and application to larger, commercially sized consignments.

B. USING THE SYSTEM IDENTIFICATION TOOLBOX

MATLAB's system identification toolbox (IDENT) is a utility which facilitates the approximation of empirical process models. The toolbox leverages a set of input/output plant data to iteratively solve the most appropriate parameters for different model structures. The model structure itself must be designed by the user, before IDENT is then able to solve for the best fitting subset of model parameters. This appendix serves as a user guide in using IDENT, by using the heat exchanger's approximate model derived in Section 6.2.2 as an example. Brief coding excerpts are given where relevant so the reader may better visualise the techniques discussed. For a look at the entire program developed for this exercise, consult the program "Data_Preparation_IDENT.m" submitted electronically.

B.1 Preparing Data For IDENT

Firstly, data must be imported into the MATLAB workspace. Being that the data in this example was contained within an Excel document, the `xlsread()` function was deployed:

```
[data, headings, raw] = xlsread('Silo22', 'B#128_Data');
```

Then to ensure compatibility with upcoming interpolation exercises, the data must be cleaned such that it contains unique data points, at unique moments in time (see Section 7.1):

```
UseData = [];  
  
filt1 = ~isnan(data(:, 11));  
filt2 = ~isnan(data(:, 12));  
  
j = 0;  
  
for i = 2 : size(data,1)  
    if data(i,1) > 0  
        if data(i,1) ~= data(i-1,1)  
            j = j+1;  
            UseData = [UseData; data(i-1,:)];  
  
        elseif (filt1(i) | filt2(i)) == 1  
            j = j+1;  
            UseData = [UseData; data(i-1,:)];  
            UseData(j,1) = 0.01 + UseData(j-1,1);  
  
        end  
    end  
end
```

```
end
end
```

In the case of this dataset, not all process values contain an entry at every time interval. This causes some values to return “Not a Number” (NaN) when imported into the MATLAB workspace. An efficient method of rectifying this is with the use of logical array operations, to filter out any NaN entries from the dataset:

```
AmbRH_Filter      = ~isnan(Ambient_RH);
AmbRH_Time        = [0; time(AmbRH_Filter); max(time)];
AmbRH_Cleaned     = Ambient_RH(AmbRH_Filter);
AmbRH_Cleaned     = [AmbRH_Cleaned(1); AmbRH_Cleaned; ...
                    AmbRH_Cleaned(length(AmbRH_Cleaned))];
```

The resulting dataset will not be regularly sampled at a consistent sample rate, which is required by IDENT in order for it to function correctly. Thus, the data must be interpolated such that sampling intervals become homogenous. For those variables which a zero order hold was necessary, a convenient MATLAB function “zoh()” was sourced online from the MathWorks file exchange [41]:

```
Ts = 60;
newTime = min(time) : Ts : max(time);

Damper_ZOH = zoh(Damper_Time, Damper_Cleaned, newTime', false)';
Ambient_RH_Interp = interp1(AmbRH_Time, AmbRH_Cleaned, newTime);
```

For this particular example, the outlet air condition of the mixing point must be solved for every time step before it can be treated as input data from the heat exchanger’s approximate model. The MATLAB function AirMixing() (submitted electronically) was created to carry out this operation:

```
for i = 1 : length(newTime)
    [RHf, Tf, Wf] = AirMixing(Ambient_RH_Interp(i),
    Ambient_Temp_Interp(i), ...
    Recycle_RH_Interp(i), Recycle_Temp_Interp(i), Damper_ZOH(i));

    RH_inlet(i) = RHf;
    T_inlet(i) = Tf;
    W_inlet(i) = Wf;
End
```

As discussed in Section 7.1 high frequency components were filtered out of the dataset to improve IDENT’s ability to find a subset of model parameters, adequately fitting the approximate model:

```
d1 = designfilt('lowpassiir', 'FilterOrder', 12, ...
    'HalfPowerFrequency', 0.01, 'DesignMethod', 'butter');
```

```
Heater_Interp_filt = filtfilt(d1, Heater_Interp);
```

IDENT is best equipped to model the *deviation* in process reactions. Thus, the dataset should be isolated if possible from steady state components and disturbances. In this case, this was executed by subtracting the inlet air disturbance from the outlet process variable. This produced a set of output data which only detailed the *deviation* of the air temperature after the inlet air had been heated; thereby concluding the preparation of input/output data:

```
Deviation = (BaseTemp_Interp - T_inlet);
Deviation_filt = filtfilt(d1, Deviation);
```

B.2 Attaining an Approximate Model with IDENT

To launch IDENT, the user must type “systemIdentification” into the MATLAB command window. This launches the IDENT graphical user interface (GUI) shown in Figure 31.

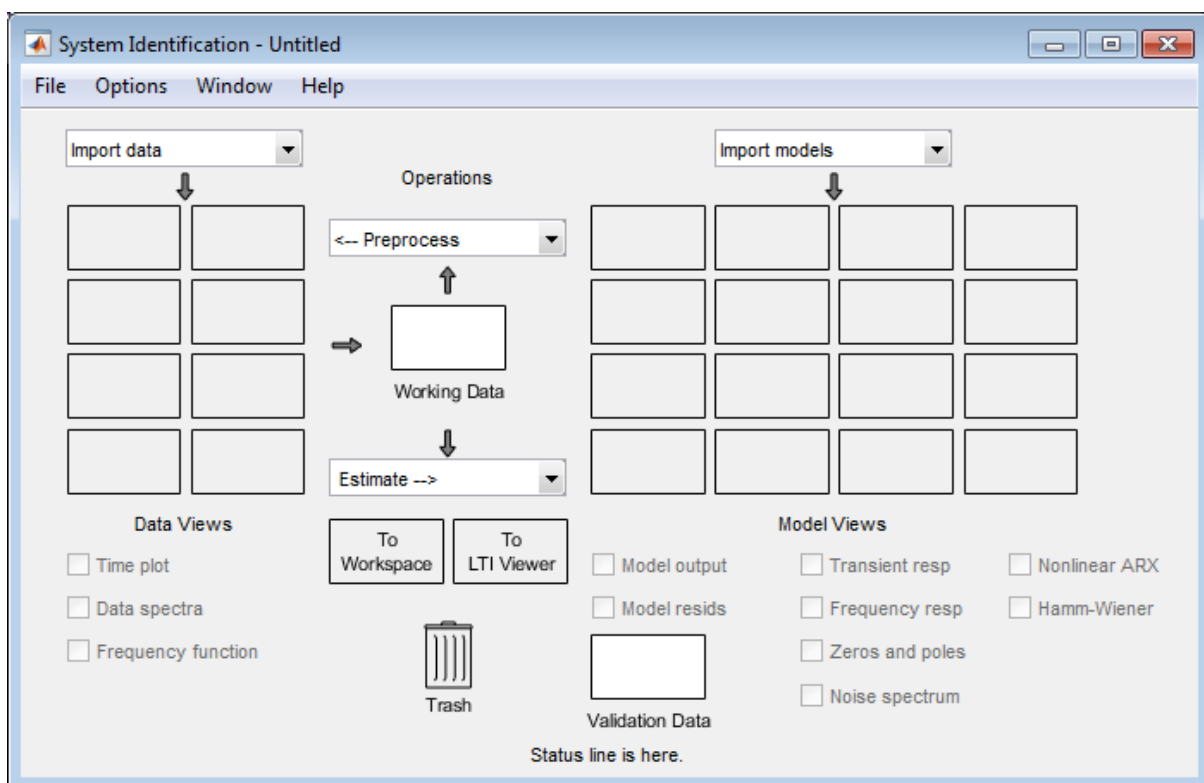


Figure 31: MATLAB system identification toolbox GUI

First, the appropriate input/output data must be imported into IDENT for use in the toolbox by launching the “Time Domain Data ...” option under the “Import Data” drop down menu. A new window will open where you can specify the name of both the input and output datasets that should already exist within the MATLAB workspace, as well as a name for the imported data, its starting time and sample time in seconds (Figure 32). Clicking “import” will extract this data from the workspace into IDENT.

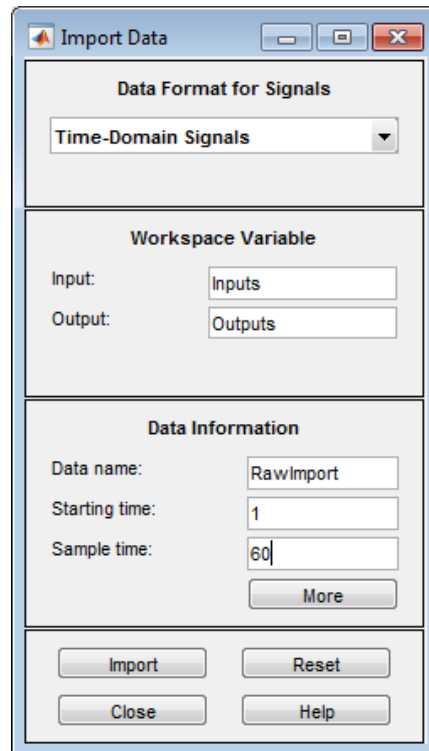


Figure 32: IDENT import data GUI

In order to ensure the modelling procedure is robust, the imported data must be split into two separate datasets. One dataset will be used for empirical model acquisition, whilst the other will be used for model validation. Splitting the data like this allows one to test any derived models against a separate set of validation data, ensuring the model doesn't only just fit that data to which it was developed from. Launch the “Select Range” window (Figure 33) from the “Preprocess” drop down menu to select a range from the original dataset to be either modelling or validation data. In this example, the first half of samples will be used as model data, and the second half will be validation data.

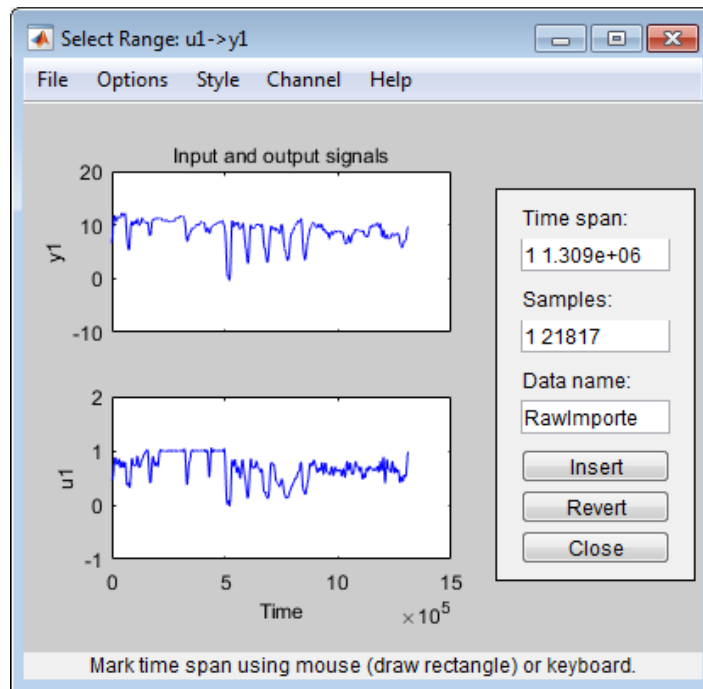


Figure 33: IDENT select range GUI

Now drag the modelling and verification datasets into the “Working Data” and “Validation Data” fields within the main GUI, as shown in Figure 31. At this point, the user can begin to experiment with different model structures as they attempt to find a suitable process model. Many different techniques can be used here to improve and refine the modelling process; a topic which is far too in-depth for the purpose of this guide. The method used to arrive at the final approximate model employed within this project and described by equation (6.12) will be given instead.

The “Process Models” window (Figure 35) was launched from the “Estimate” drop down menu, which facilitates the creation of various linear transfer function model structures. Various structures were attempted, with the most suitable being a system with two real poles, one zero and no delay. There are various ways to view the output of the process model to determine its accuracy. The best of which is to launch the “Model Output” window (Figure 34) from the main GUI to compare how different models are performing against the validation dataset. Once a suitable model has been created, it may be viewed in detail and exported to the workspace by double clicking on its icon in the main IDENT GUI.

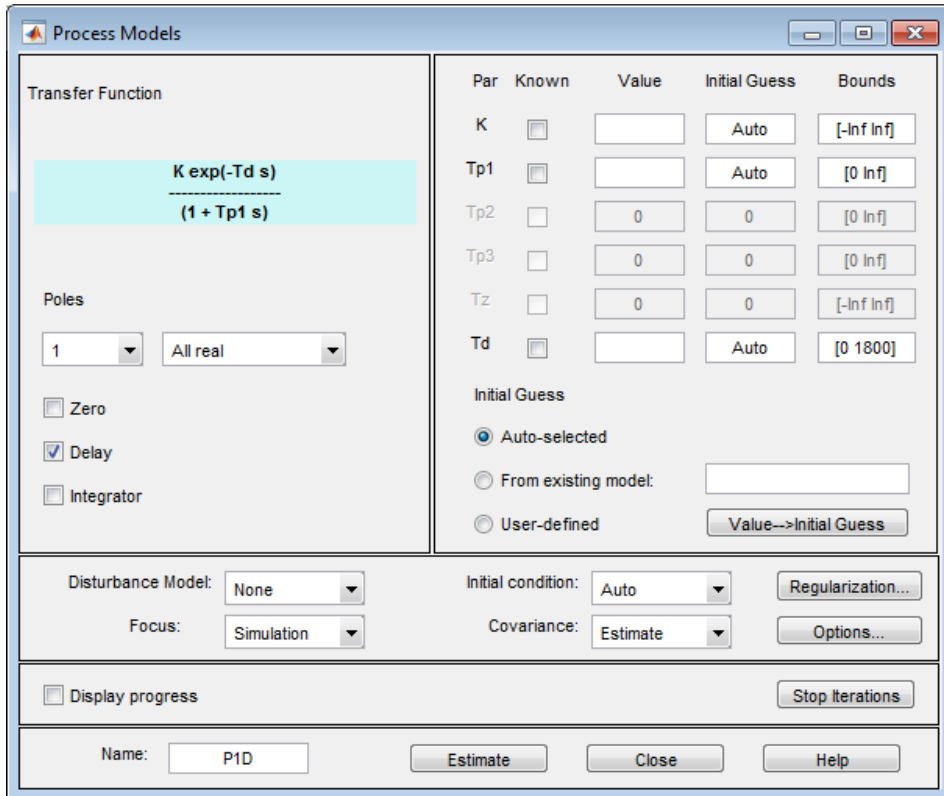


Figure 35: IDENT process models GUI

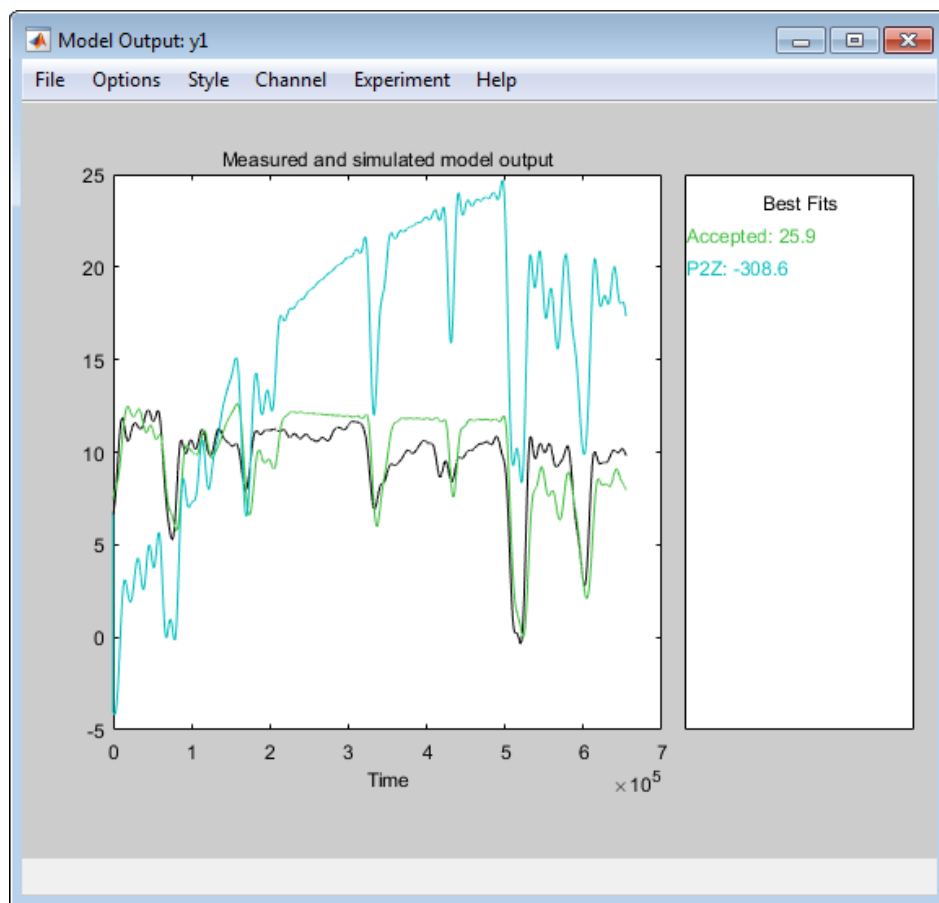


Figure 34: IDENT model output GUI

C. APPROXIMATING THE EQUIVALENT DRYING TIME

It was mentioned in Section 6.3.1 that the simulation broke down when trying to run the `fzero()` MATLAB function during the verification procedure. This appendix details the workaround used to approximate the equivalent drying time to avoid such errors. Since the `fzero()` method worked under purely simulated conditions, it was possible to plot and analyse how the equivalent drying time (t_{eq}) varied over time. Figure 36 depicts how t_{eq} varies across different regions in the nut bed for a “typical” drying run under simulation.

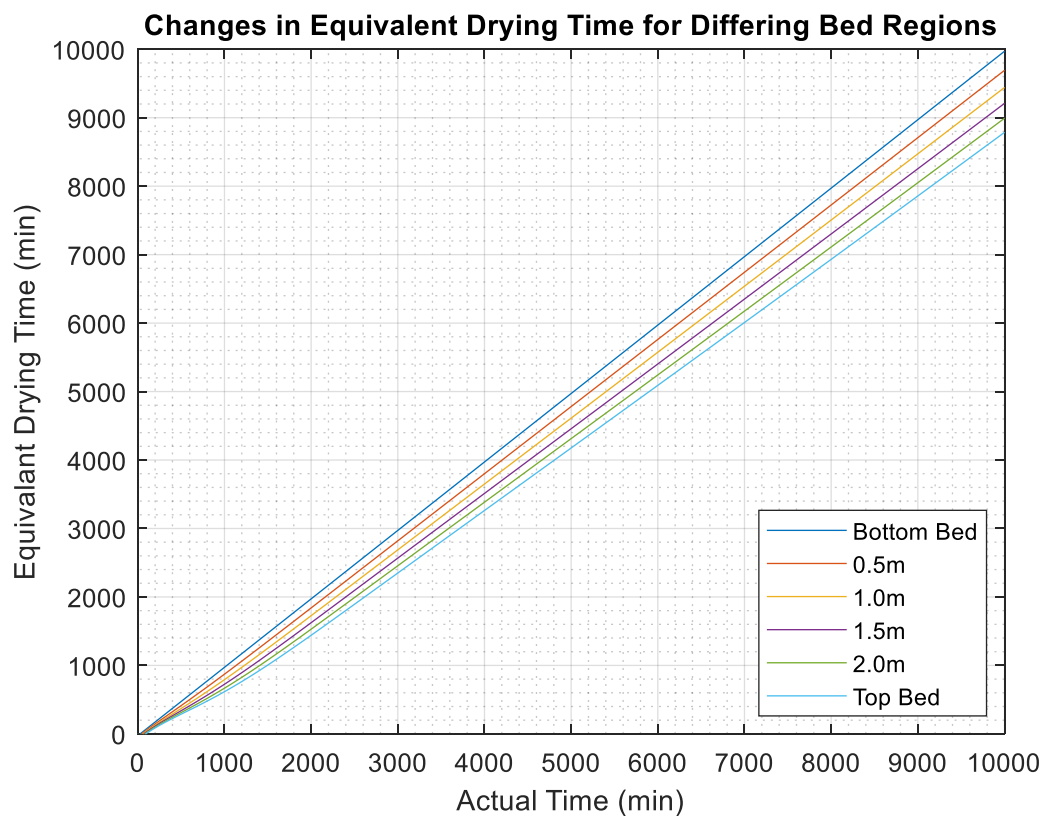


Figure 36: Changes in equivalent drying time over actual drying time

Intuitively, the bottom bed layer’s equivalent drying time is simply equal to that of the actual drying time, since there is no lag in drying experienced at this position. But as the focus shifts to regions above, the equivalent drying time begins to slightly lag that of the actual time, due to the upper layers drying slower than the lower. The trends in Figure 36 are relatively linear, with the lag experienced between regions being somewhat constant across all regions for any given point in time. The method used to recreate this effect – without the use of the `fzero()` function – was to find the difference in

equivalent drying time between the top and bottom layers, before finding a linear relationship that calculates how much this quantity should vary for different bed regions. In truth, two separate approximations were calculated for different drying intervals, to capture the initial dynamics evident in Figure 36 up to approximately 1500 seconds. Figure 37 shows the exercise, with the initial piecewise linear approximation being explicitly written in equation (8.1).

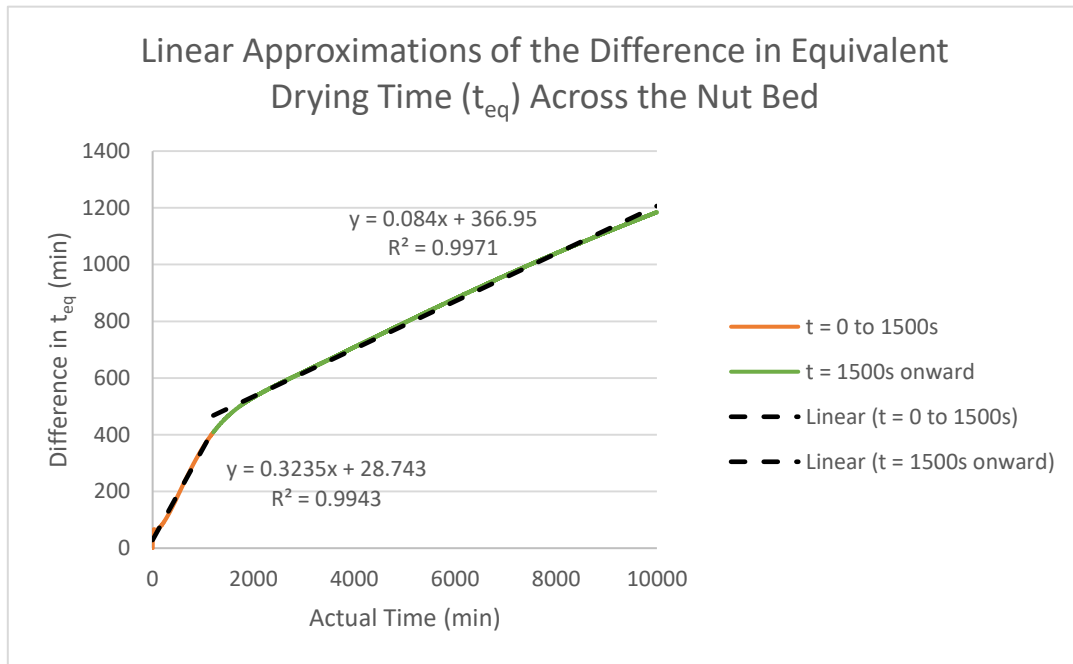


Figure 37: Piecewise linear approximation of changes in equivalent drying time

$$\Delta t_{eq (Bottom \rightarrow Top)} = \begin{cases} 0.3235t + 28.743, & t \leq 1500s \\ 0.084t + 366.95, & t > 1500s \end{cases} \quad (8.1)$$

If this piecewise approximation is said to be the difference in equivalent drying time across the entire bed, then any incremental layer within the bed will be given as:

$$\Delta t_{eq (Bottom \rightarrow Layer(i))} = \begin{cases} \frac{i(0.3235t + 28.743)}{N - 1}, & t \leq 1500s \\ \frac{i(0.084t + 366.95)}{N - 1}, & t > 1500s \end{cases} \quad (8.2)$$

Where i is the layer index (starting from zero), and N is the total number of layers considered in the simulation. It should be noted that the equivalent drying time can indeed be negative, as this implies a moisture gain by the product instead of a moisture loss. Using this approximation, the simulation

would no longer crash when attempting validation against plant data. The `fzero()` method of solving t_{eq} is still deployed for purely simulated tests.